Research Paper

A new promising anticancer agent: a glycosaminoglycan-mimetic derived from the marine bacterial infernan exopolysaccharide

Dominique Heymann[1,2,3,#,*], Javier Muñoz-Garcia[1,2,#], Antoine Babuty[1,2,4,#], Antoine Audéon[2,5], Emilie Ollivier[2], Dulce Papy-Garcia[6], Sandrine Chantepie[6], Agata Zykwinska[7,#], Corinne Sinquin[7,#], Sylvia Colliec-Jouault[7,#,*]

[1]Nantes Université, CNRS, UMR6286, US2B, F44322, Nantes, France

[2]Institut de cancérologie de l'Ouest, Tumor Heterogeneity and Precision Medicine laboratory, F-44805, Saint Herblain, France

[3]University of Sheffield, School of Medicine and Population Health, S102RX, Sheffield, UK

[4] CHU de Nantes, Department of Hemostasis, F-44201, Nantes, France

[5]SATT Ouest Valorisation, F-44201, Nantes, France

[6] Université Paris Est Créteil (UPEC), Glycobiology, Cell Growth and Tissue Repair Research Unit (Gly-CRRET), F-94010 Créteil, France.

[7]Ifremer, MASAE Microbiologie Aliment Santé Environnement, F-44000, Nantes, France

# These authors contributed equally to the present work

*Corresponding authors:

Prof. Dominique Heymann; Institut de Cancérologie de l'Ouest, Blvd Jacques Monod, 44805 Saint-Herblain, France. E-mail : dominique.heymann@univ-nantes.fr, Tel.: +33-240 679 841.

Dr. Sylvia Colliec-Jouault; Ifremer Centre Atlantique, BP 21105, 44311 Nantes Cedex 03, France. E-mail : Sylvia.Colliec.Jouault@ifremer.fr; Tel.: +33-240 374 093.

26

Abstract

Marine microorganisms are a promising source of innovative compounds for medical applications. The present study aimed to investigate anticancer potential of oversulfated low molecular weight derivatives, named OSIDs, prepared from infernan, a marine bacterial exopolysaccharide. In order to identify a lead, OSIDs with different sulfate contents and molecular weights were firstly evaluated *in vitro* in a large series of human and murine tumor cell lines. Amongst all derivatives tested, OSID4 was the most effective, showing a significant dose-dependent inhibitory effect on the viability of cancer cells. OSID4 was then able to significantly slow down progression of lung and melanoma tumor growth in immunocompetent tumor-bearing mouse models. In immunodeficient mice bearing a human lung carcinoma, a notable inhibitory effect of OSID4, comparable to doxorubicin, was observed. In combination with doxorubicin, OSID4 did not exhibit any drug interaction. The activity of OSID4 was confirmed by its modulatory effect on the transcriptomic profile of human lung cancer cells. Finally, toxicity and pharmacokinetic parameters disclosed that OSID4 presented no toxicity and no bleeding risk. In conclusion, by combining its notable anticancer and moderate anticoagulant activities, OSID4 may be promising for treatment of cancers associated with a high risk of thromboembolic events.

Keywords: exopolysaccharide, GAG-mimetic, antitumor, allograft mouse model, xenograft mouse model, drug combination, toxicity, bleeding, thromboembolism

1. Introduction

Cancer is among the leading causes of mortality in developed countries with major economic impact [1, 2]. Despite the endeavors and achievements made in treating cancers during the past decades, disease recurrence and progression remain a major obstacle to therapy. One of the main clinical issues is the development of drug resistance [3]. Many strategies have been designed to combat drug resistance, either by combining the currently available therapies or by developing novel therapies [4]. While the focus is shifting to the development and use of novel therapeutic agents for immunotherapy and targeted therapy, chemotherapy remains the standard of care for the treatment of most cancers and both new and effective chemotherapeutic agents are still needed. However, systemic chemotherapy induces severe side effects, has a low tumor specificity and has more a survival effect than a curative impact with a poor improvement of quality of life [5, 6]. Moreover, the incidence of venous thromboembolism (VTE) in cancer patients has strongly increased in the past decade probably due to the novel cancer therapies targeting more distant metastasis by using antiangiogenic therapy [7]. Prior to cancer surgery, pharmacological thromboprophylaxis with low-molecular-weight (LMWH) or unfractionated (UFH) heparin is the standard of care for patients with both a high risk of VTE and a low risk of bleeding [8]. However, the potent anticoagulant activity of LMWH and direct oral anticoagulants leads to adverse bleeding complications in some cancer patients, which limits their period of administration (up to 6 months), as shown in recent clinical studies [9].

Glycosaminoglycans (GAGs), and especially heparins, are until now considered as good therapeutic candidates in oncology due to their multi-target mechanisms of action (e.g. growth factors, chemokine signaling, angiogenesis, distant metastasis) [10]. In this context, the therapeutic potential of heparins in cancer patients has been evaluated to improve their overall survival. However, besides their strong anticoagulant activity another disadvantage of

heparins is their animal origin, which can lead to a high risk of unknown cross-species contamination [11-13]. Consequently, the exploration of the therapeutic potential of heparin mimetics or analogs is booming. Through their weak anticoagulant activity by inhibiting not only thrombin generation, fibrin formation but also heparanase (enzyme involved in heparan-sulfate metabolism and turnover), heparin analogs are often less anticoagulant than heparins and exhibit potential antimetastatic activities [14, 15]. These analogs, *via* a multi-target mechanism of action have inhibitory effects on heparanase, selectins, growth-factor receptor signaling with limited side effects. Sulfated oligosaccharides have been studied, such as a sulfated form of phosphomannopentaose and phosphomannotetraose named PI-88 (muparfostat) but also a sulfated tetrasaccharide derivative named PG545 (pixamitod) and a glycol-split *N*-acetyl heparin derivative SST0001 (roneparstat) [16]. Among heparin analog drugs, PG545 is well tolerated [17] and this compound is still ongoing clinical trial. In clinical phase I trial SST0001 (roneparstat) did not show any direct anticancer effect [10].

In recent years, there has been a growing interest in isolation and identification of natural molecules that can replace animal products (e.g. heparins) and might have new applications in pharmaceutical industry and particularly in oncology [18, 19]. Microbial polysaccharides compete with polysaccharides from other sources such as animals, higher plants, algae, microalgae or fungi [20-26]. Interest in mass culture of microorganisms from marine environment has increased considerably, representing an innovative approach to biotechnological use of under-exploited resources. When sulfated, bacterial anionic polysaccharides from different microorganisms can share some biological properties with GAGs and especially heparins, without exhibiting the same bleeding risk and with a low risk of contamination by a non-conventional transmissible agent such as prions or emerging viruses due to a large “species-barrier” [27-29]. Marine bacteria associated with deep-sea hydrothermal conditions have demonstrated their ability to produce, in an aerobic

carbohydrate-based medium, unusual extracellular polysaccharides or exopolysaccharides (EPS). They present original structural features that can be modified to design bioactive compounds and improve their specificity [30, 31]. In particular, an EPS, recently named infernan and produced by a deep-sea hydrothermal bacterium assigned *Alteromonas infernus* (GY785 strain), presents a very complex structure. Infernan EPS chains are all composed of branched disulfated octasaccharide repeating units providing a homogeneous structure unlike most other natural polysaccharides [32, 33]. Chemical modifications (depolymerization and sulfation) of infernan EPS have been undertaken with the aim of promoting biological activities. Indeed, highly oversulfated LMW infernan derivatives (called OSIDs) have shown previously multiple biological properties. In particular, an infernan derivative of 24 kDa and 40 wt% sulfate, tested in clotting assays, was found to be 10 and 2 times less active to prolong clotting time than UFH and LMWH, respectively. In activated partial thromboplastin time, the same anticoagulant effect was obtained for the 24 kDa infernan derivative, UFH and LMWH with respectively a concentration of 10, 1.5 and 4 µg/mL [34]. Another highly sulfated LMW infernan derivative of 15-20 kDa named OSID1 displayed antimetastatic properties. The *in vivo* experiments showed no effect on the primary osteosarcoma tumor growth but OSID1 was very efficient to inhibit the establishment of lung metastases in a mouse model receiving murine osteosarcoma cells [35].

In this context, the objective of the present study was to explore for the first time whether OSIDs, presenting different molecular weights (Mws) and different contents of sulfate groups, could directly inhibit *in vitro* and *in vivo* cell proliferation and tumor growth of a large series of human and murine cancer cell lines. As well described for sulfated polysaccharides, both sulfate content and Mw are key parameters that can modify their mechanism of action. Multidrug therapy, based on the administration of at least two agents with often various mechanisms of action (e.g. polychemotherapy, chemotherapy and

immunotherapy), became progressively treatments of reference in numerous oncological entities [36]. In this context, OSID effect in tumor bearing mice was investigated alone or in combination with doxorubicin, a chemotherapeutic agent frequently used in oncology. Complementary functional studies were carried out *in vitro* to better understand the biological activities of these derivatives on cancer cells. Finally both toxicity and pharmacokinetic studies were conducted in murine models to evaluate the potential risks and side effects for future pre-clinical and clinical studies.

2. Materials and Methods

2.1. Preparation and characterization of infernan derivatives

The bacterial EPS, named infernan, was produced by fermentation of *Alteromonas infernus* (strain GY785), a deep sea aerobic, mesophilic and heterotrophic marine bacterium isolated in the vicinity of an active hydrothermal vent of the Guaymas Basin (Gulf of California) during the Guaynaut cruise in 1991. Soluble native high Mw (HMW) infernan EPS was isolated from culture medium by high speed centrifugation, purified by frontal filtration, concentrated by ultrafiltration, freeze dried and characterized as previously described [37]. The preparation, purification and characterization of highly oversulfated LMW infernan derivatives (OSIDs) were performed as previously reported [38, 39]. Briefly, native HMW EPS was depolymerized first using a free-radical depolymerization process to obtain LMW EPS with different Mws. Copper (II) in aqueous solution was added with stirring to HMW EPS dissolved in water at 60°C and pH 7.5; then diluted hydrogen peroxide was added. After depolymerization step, LMW EPS chains were reduced with sodium borohydride, purified on Chelex® resin, ultrafiltered and freeze dried. LMW EPS, in a pyridinium salt form, were then oversulfated in dimethylformamide (DMF) using pyridine sulfate as sulfating agent leading to obtain oversulfated LMW EPS derivatives (OSIDs). First 100 mg of LMW EPS in its pyridinium salt form was solubilized in extra dry DMF over

148 molecular sieve (20 mL) for 2h at 45°C under continuous stirring and then sulfated for the
149 next 2h at 45°C in the presence of pyridine sulfate. The final aqueous solution (pH 7) was
150 dialyzed against water for three days before freeze-drying. Mws before and after sulfation
151 were determined by HPSEC-MALS and sulfur content (wt% S) by HPAEC chromatography
152 [38, 39]. Heparin and Dalteparin were purchased from Sigma Aldrich (Saint-Quentin
153 Fallavier, France).

154 *2.2. Tumor cell lines and cell culture*

155 All experiments were conducted at 37°C in a humidity-saturated controlled atmosphere
156 and 5% CO_2. All human tumor cell lines used in the present study were obtained from the
157 American Tissue Cell Collection (ATCC, Molsheim, France) and were mycoplasma free.

158 *Adherent human cell lines*: MNNG/HOS osteosarcoma, A375 melanoma, $CaCO_2$ colon
159 cancer and DU145 prostate adenocarcinoma lines were cultured with DMEM 4.5 g/L high
160 glucose (Sigma Aldrich), pyruvate, non-glutamine from Gibco (Thermo-Fisher, Saint-
161 Herblain, France). LnCap prostate adenocarcinoma cell line was expanded in RPMI1640
162 (Sigma Aldrich). A549 non-small cell lung cancer cell line was cultured with DMEM/F12
163 (Sigma Aldrich, Saint-Quentin Fallavier, France). MDA-MB-231 breast carcinoma cell line
164 was cultured with L-15 media from Gibco. All culture media were supplemented with
165 glutamine and 5% of FBS.

166 *Adherent murine cell lines*: MOS-J osteosarcoma cell line was provided by Dr Shultz [40].
167 4T1 mammary cancer, CMT-167 lung cancer and B16-F10 melanoma cell lines were
168 purchased from ATCC. All mouse cell lines were cultured in DMEM supplemented with
169 glutamine and 5% of FBS.

170 *2.3. MTT cell viability assay*

171 Cell viability assay was performed by seeding 3,000 cells of each cancer cell line per well
172 for 4 hours at 37°C in a 96-multiwell plate before adding increasing doses of OSIDs (from 1

µg/mL to 1 mg/mL). Each plate was incubated at 37°C in a humidity-saturated atmosphere and 5% CO_2 for 72 hours. After 3 days of treatment, a volume of 10 µL of 5 mg/mL MTT (Sigma-Aldrich) per well was added and incubated for 3 hours at 37°C under 5% CO_2 [41]. The supernatants were then removed and 200 µL per well of DMSO were added to dissolve the formed formazan crystals before proceeding to the colorimetric quantification by spectrophotometry (Victor 3x, PerkinElmer, Villebon-sur-Yvette, France) at the wavelength of 500-600 nm. Experiments were done in triplicate and repeated twice.

2.4. Real-time cell proliferation assay

Cell proliferation was analyzed by xCELLigence technology (Agilent, Les Ulis, France) as previously described [42]. Background was measured by adding 50 µL of corresponding media into an E-Plate view 96 (Agilent). Before the beginning of treatment, cells were seeded in triplicate at 5,000 cells per well (50 µL) for 4 hours at 37°C before adding increasing concentrations of OSIDs (from 1 to 500 µg/mL). The choice of these concentrations for each particular cell line was determined as a function of the IC_{50} established by the MTT assay. Proliferation curves were normalized with respect to the time point of drug incorporation. The plate was monitored for 5 days using a RTCA instruments (Agilent) using a RTCA device (Agilent). Experiments were done in triplicate and repeated twice.

2.5. NanoString™ analysis

Transcriptomic profile of the human A549 lung adenocarcinoma cells line was assessed in the presence or the absence of 100 µg/mL of OSID4 for 24 hours by NanoString technology as previously described [43]. Briefly, RNA from treated and untreated cells was extracted using Macherey-Nagel's NucleoSpin RNA Plus XS kit (Macherey-Nagel, Hoerdt, Allemagne). RNA concentration was quantified on a NanoDrop. For NanoString™ analysis, 50 ng of RNA in a maximum volume of 5 µL was required per sample. Cell messenger RNAs were extracted and a differential analysis of 814 genes (NH_Hs_TumorSig_v1.0) was

198 performed by NanoString technology. Hybridization of capture and reporter probes with
199 target RNAs was performed according to the manufacturer's recommendations. The solution
200 containing the RNA samples and probes was placed in a thermocycler at 65°C for at least 16
201 hours. Following hybridization, the samples were put in an automated nCounter Prep Station
202 to remove excess probes and mRNA. The purified samples were then loaded onto a cartridge,
203 where they could bind via the biotin of the capture probe. The fixed samples were then loaded
204 into a second automated system, the nCounter Digital Analyze, a multi-channel
205 epifluorescence scanner. The scanner took as many images as the number of reporter probes
206 detected. These images were then converted into digital values for analysis. The data obtained
207 were analyzed using NanoString nSolver Analysis Software, and statistical tests were
208 performed. The experiments were conducted in triplicate.

209 *2.6. Tumor models in immunocompetent and immunodeficient mice*

210 All procedures involving mice were conducted in accordance with EU Directive
211 2010/63/EU for animal experiments after reviewing and validation by the institutional
212 guidelines of the French Ethical Committee (CEEA-6-PDL, agreement APAFlS#28216-
213 2020111915429758v6). Mice were housed under pathogen-free conditions in Atlanthera
214 Preclinical Center (Saint-Herblain, France). Melanoma and lung cancer models were induced
215 in 8 week-old female C57/BL6 and NMRI nude mice (Charles River, Ecully, France). Both
216 oncological entities being hormone-independent, cancer cells were inoculated in females
217 which are easy to maintain than males. 500 x 10^3 mouse CMT167 (n = 8-9 mice per group) or
218 100 x 10^3 mouse B16F10 (n = 5-6 mice per group) cell suspension in Matrigel^{TM} were
219 inoculated subcutaneously in the right flank of C57/BL6 immunocompetent mice. Similarly,
220 10^6 human A549 cells were injected subcutaneously in nude mice. For cell injection and
221 tumor monitoring, mice were anesthetized by inhalation of isoflurane at 2% in air with a flow
222 of 1 L/min. OSID4 (Mw 60 kDa and sulfate content 40 wt%) showing the best *in vitro* effect

was evaluated *in vivo*. Mice were then distributed randomly in 2 groups of control and treated groups. The dose of OSID4 used referred to the previous work carried out on osteosarcoma [35]. OSID4 was injected by subcutaneous route at a dose of 10 mg/kg per day (treated group), five times a week and compared to a solution of NaCl (control group). The treatment started 3 days post inoculation of cancer cells.

OSID4 combined to doxorubicin was assessed in human A549 non-small cell lung cancer *in vivo* mouse model (n = 6 mice per group). Nude mice were then distributed randomly in 4 groups of 8 mice allocated at the following treatments: i) Control group: NaCl by subcutaneous route 5 times a week; ii) OSID4 group: 4 mg/kg by subcutaneous route 5 times a week; iii) Doxorubicin group: 3 mg/kg by intravenous route 3 consecutive days (cumulative dose showing no cardiotoxicity [44]); iv) Combined group: doxorubicin 3 consecutive days + OSID4 5 times a week. Sixty-four mice were used in the present study. The treatment started 3 days post inoculation of cancer cells. The weight of the animals and the tumor volume measured with a caliper were monitored twice a week. Tumor volume (V) was calculated using the formula: length × width × depth × 0.5 [45]. Mice under anesthesia (see description above) were sacrificed by cervical dislocation.

2.7. Pharmacokinetic studies

Studies to obtain pharmacokinetic data on OSID4 was carried out. These studies were conducted by the "Glyco-mix" platform of the University of Paris Est Créteil (UPEC, Créteil, France). All aspects of this work, including housing, experimentation, and disposal of animals were performed in general accordance with the European Guidelines for the Care and Use of Experimental Animals. The animal care and used protocols were reviewed and approved with agreement number #19838 by the SBEA ethics committee of the University Paris Saclay, France. All animals were 4 week-old male SWISS mice weighing 20 $\pm$ 2 g provided by Laboratoires Janvier (Le Genest, St. Isle, France). The choice of male mice is in accordance

with the principle of "3Rs alternatives" (reduction, refinement and replacement). In brief, the quantification of OSID4 was carried out using a colorimetric assay specific for sulfated molecules of GAG type [46, 47]. The OSID4 was detectable and quantifiable with good linearity in an aqueous solution at concentrations from 12.5 to 250 µg/mL and in plasma at concentrations from 6.3 to 100 µg/mL. The OSID4 was also detectable in plasma by its anticoagulant activity by measuring the inhibition of Factor Xa activity using anti-Xa chromogenic assays [48]. The conversion of Xa factor activity to IU/mL was performed by considering that 0.19 IU is equivalent to 1 µg of factor Xa as it mentionned in the instructions provided by Diagnostica Stago laboratories. Two pharmacokinetic studies were conducted in male mice on OSID4: one study with an injection by intravenous route at 10 mg/kg and another one with an injection by subcutaneous route at 30 mg/kg. After intravenous administration, blood was collected at different time points following the injection: 15, 60, 120, 180 and 240 minutes (groups of 5 mice *per* time point + 5 control mice 15 minutes after NaCl solution injection), and the concentration of OSID4 in mice plasmas was determined. After subcutaneous administration, blood was collected at different time points after the injection: 30, 60, 90, 120, 180, 240, 480 and 1440 minutes (groups of 5 mice *per* time point). The concentration of OSID4 in plasma was evaluated at the different time points and compared to result obtained in plasma from control mice (n = 5) 30 minutes after subcutaneous injection of a NaCl solution. At the end of the experiment, mice under anesthesia (see description above) were sacrificed by cervical dislocation.

2.10. Toxicological study

A toxicity study was performed using a mouse model by intravenous injection of OSID1 or OSID4 at doses of 10, 30 and 100 mg/kg. This study was conducted by Eurofins Discovery Partner Lab. All aspects of this work, including housing, experimentation, and disposal of animals were performed in general accordance with the Guide for the Care and Use of

Laboratory Animals: Eighth Edition (National Academy Press, Washington, D. C., 2011) in AAALAC-accredited laboratory animal facility. The animal care and use protocol were reviewed and approved by the IACUC at Pharmacology Discovery Services Taiwan, Ltd. A 14 day toxicity study was performed following OSID administration every other day for 3 days (day 1, 3 and 5) in male and female ICR mice (group of 4 males + 4 females per dose and control). Body weights, clinical observations and mortality were recorded from days 1 to 14. On day 14, all animals were necropsied for histopathological analysis of 6 organs (heart, lung, brain, kidney, spleen and liver). Mice under anesthesia (see description above) were sacrificed by cervical dislocation.

2.11. Statistical analyses

Independent experiments have been done in triplicate and data are given as a mean ± SD. Results were considered significant at p values ≤ 0.05, p values ≤ 0.01 and p values ≤ 0.001. Corresponding groups were compared using Tukey's HSD test. The data analysis for this paper was generated using the Real Statistics Resource Pack software (Release 8.9.1). Copyright (2013 – 2023) Charles Zaiontz. www.real-statistics.com.

For pharmacokinetic studies, data were presented as means ± SD of five independent experiments. Data were analyzed by one-way analysis of variance (ANOVA), and the student's t test were used to determine the level of significance of differences; a significant difference was accepted from $p < 0.05$.

3. Results and discussion

3.1. Characteristics of infernan derivatives

Different productions of infernan EPS by fermentation of *Alteromonas infernus* have been conducted at laboratory and pilot scales (from 1- to 20-L fermenters) at 25 °C, neutral pH, under atmospheric pressure in Zobell medium supplemented in glucose (30 g/L). The EPS isolated after each fermentation was produced with a yield close to 4 ± 1 g/L without any batch

variability. The structure of native infernan EPS has been totally described, its repeating unit is a branched disulfated octasaccharide presenting 3 adjacent uronic acids (one galacturonic acid and two glucuronic acids) and 2 sulfate groups (at O-2 of galacturonic acid of the main chain and at O-6 of terminal galactose in the side chain) as presented in Fig. 1 [32, 33]. Recent NMR analysis allowed to determine that sulfate groups are distributed in both backbone and side chain of OSIDs with all primary hydroxyl groups substituted with sulfate groups (Fig. 1). After modifications, the OSIDs showed unchanged repeating unit [49].

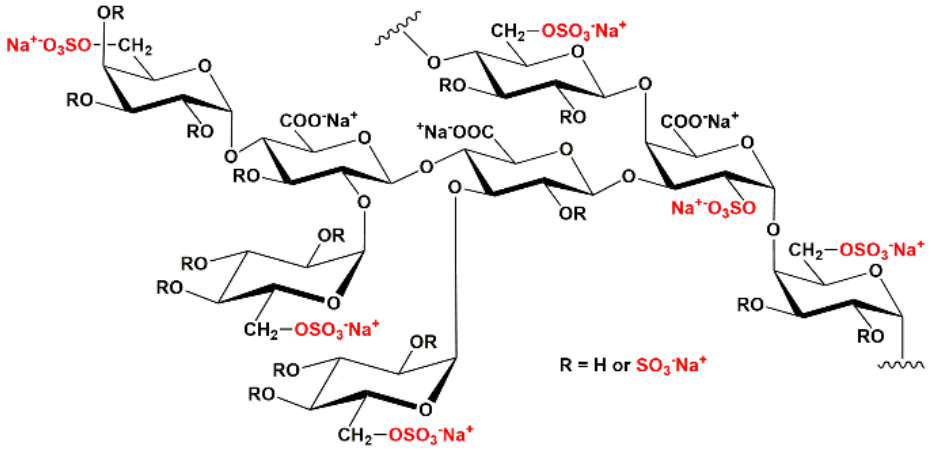

Fig. 1. Octasaccharide repeating unit of infernan EPS. Sulfated positions in LMW sulfated derivatives are indicated in red [49].

A previous study showed that OSID1 (15 kDa and 40 wt% sulfate) was very efficient to inhibit *in vivo* establishment of lung metastases without any effect on the primary osteosarcoma tumor, a bone tumor presenting a high potency to induce lung metastases [35]. With the aim of exploring if OSIDs could have an effect on the tumor growth in different types of cancer such as lung, breast, colon, prostate and skin cancers, four OSIDs presenting various Mws and sulfate contents were prepared and characterized (Table 1). Among different derivatives, OSID1 had both Mw and sulfate content close to those of heparin whereas OSID2, OSID3 and OSID4 displayed a three-fold higher Mw with increasing sulfate contents 10, 20 and 40 wt%, respectively.

Table 1: Characterization of oversulfated infernan derivatives (OSIDs) and two commercial heparins.

Name	Mw Da	I Mw/Mn	Sulfate % (w/w)
OSID1	20,000	< 2	40
OSID2	60,000	< 2	10
OSID3	60,000	< 2	20
OSID4	60,000	< 2	40
Heparin (UFH)	15,000	np	30
Dalteparin (LMWH)	5,000	np	30

Mw: weight-average molecular weight; Mn: number-average molecular weight; I: dispersity; np: not provided by manufacturer.

3.2. In vitro effects of four OSIDs on a panel of human cancer cell lines

3.2.1. OSIDs modulate cancer cell viability and proliferation

The *in vitro* effect of the four OSIDs, compared to heparin and dalteparin (control compounds), on both viability and proliferation of cells for five human tumor cell lines were evaluated by MTT assay and xCELLigence technology, respectively. The results on cell viability for human osteosarcoma and human lung cancer were presented in Fig. 2 and 3, respectively. Both heparin and dalteparin did not show any inhibitory effect on the viability of MNNG-HOS human osteosarcoma cell line (Fig. 2). Conversely, an inhibitory effect was observed for all OSIDs, the most important effect on cell viability was found with OSID4 in a dose-dependent manner. The same results were obtained on A549 human non-small cell lung cancer cell line (Fig. 3). For both human cell lines treated with OSID4, 40% of inhibition of cell viability were noted at a concentration of 100 µg/mL and a strong inhibition (≥80%) above 500 µg/mL, pointing a moderate sensibility after 3 days of treatment.

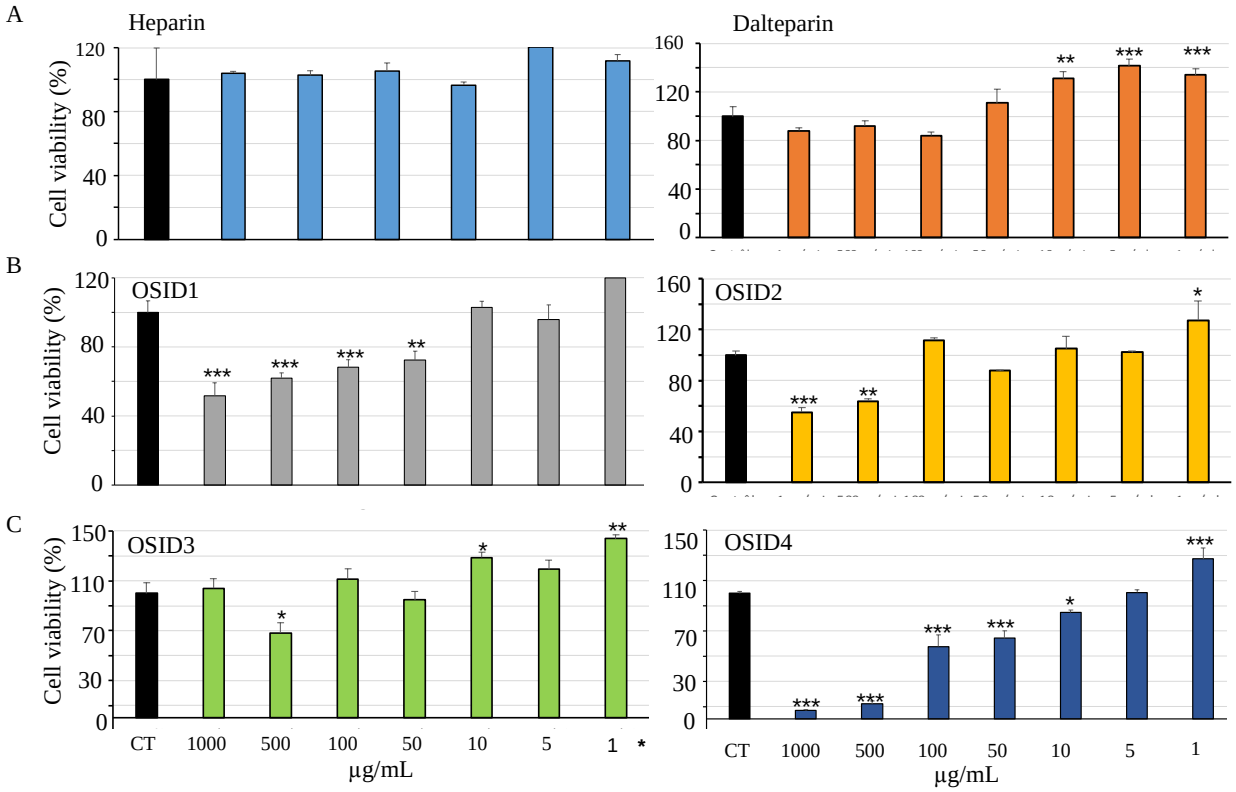

Fig. 2. Effect on the viability of MNNG-HOS human osteosarcoma cell line measured by MTT assay. (A) Heparin and dalteparin. (B) OSID1 and OSID2. (C) OSID3 and OSID4. *p< 0.05; **p<0.01; ***p<0.001.

The viability of the other human cell lines treated 3 days with OSID4 was either slightly inhibited (colon cancer, breast cancer and melanoma) or inhibited without a clear dose-response (prostate cancers) (Fig. S1). The effect of OSIDs was also evaluated on various murine cancer cell lines (mammary, lung cancers, melanoma and osteosarcoma) and similar results to those observed on human cells were obtained (Fig. S2).

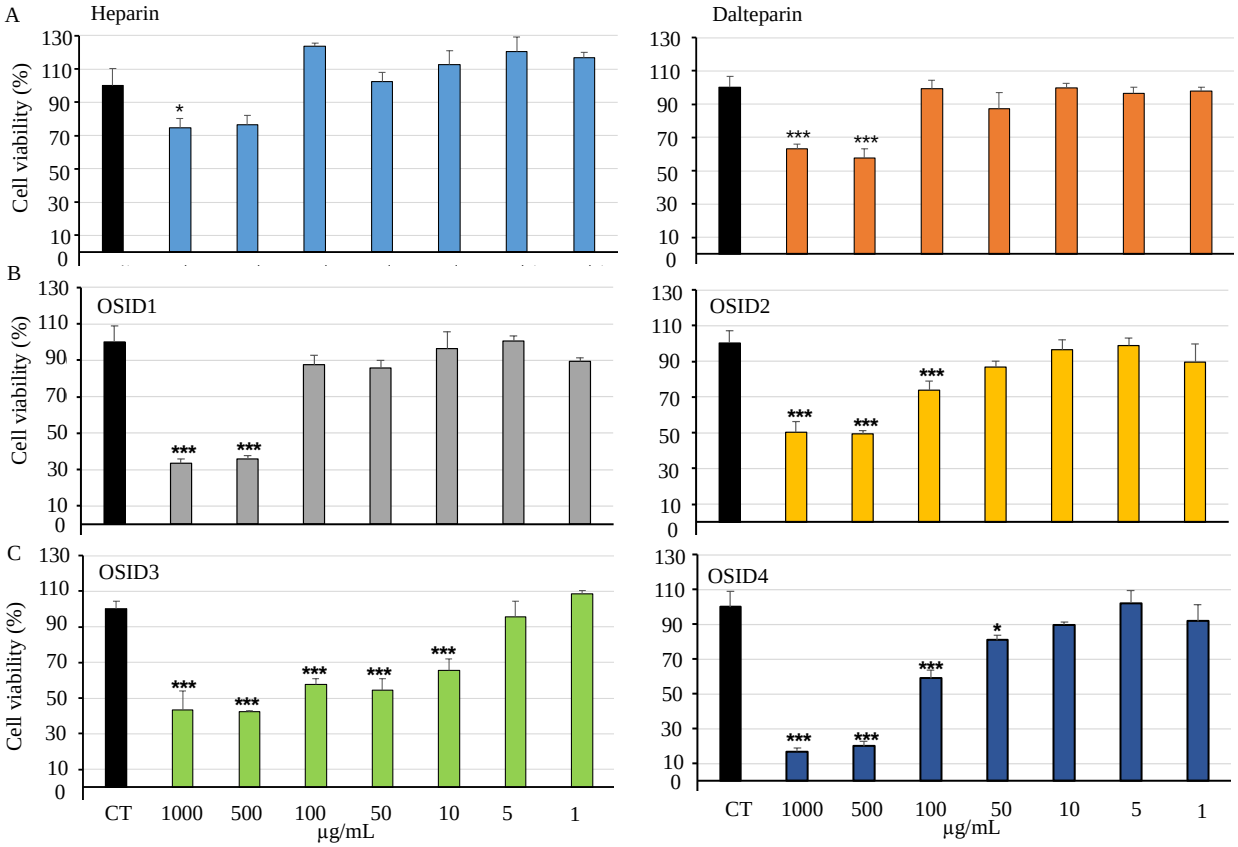

Fig. 3. Effect on the viability of A549 human non-small cell lung cancer cell line measured by MTT assay. (A) Heparin and dalteparin. (B) OSID1 and OSID2. (C) OSID3 and OSID4. *p< 0.05; **p<0.01; ***p<0.001.

The results on cell proliferation for human prostate cancer and human osteosarcoma were presented in Fig. 4. After more than 4 days (> 100 hours) of treatment with OSID4 a total inhibition of cell proliferation was obtained for human prostate cancer and human osteosarcoma cell lines at doses of 25 µg/mL and 500 µg/mL, respectively. OSID4, presenting both the highest Mw and sulfate content, was the most potent derivative to inhibit cell viability and proliferation. OSID4 exhibited a remarkable inhibitory effect on proliferation of human prostate cancer cells at relatively low concentrations (below 50 µg/mL). Compared to OSID1, displaying 3-times lower Mw but the same sulfate content, OSID4 exhibited a more pronounced activity as shown on DU145 human prostate cancer cells (Fig. S3).

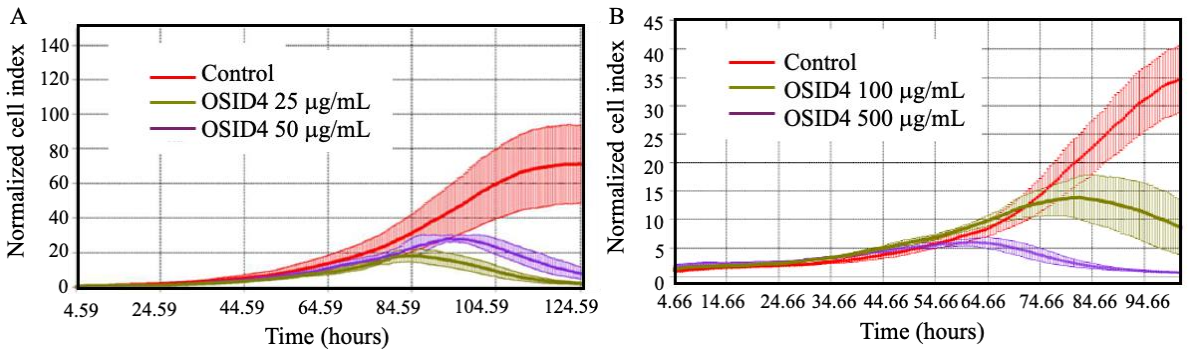

Fig. 4. OSID4 reduced significantly proliferation of cancer cells in a dose-dependent manner. (A) DU145 human prostate cancer cells. (B) MNNG-HOS human osteosarcoma cells. Cells were seeded in triplicate at 5,000 cells per well (E-Plate view 96) for 4 hours prior to the addition of increasing doses of OSID4. Cell proliferation was followed by real-time measurement of cell impedance using xCELLigence technology (RTCA Instruments). Proliferation curves were normalized to the time of drug incorporation. Experiments were performed in triplicate and repeated twice.

Similar results were reported for chemically oversulfated polysaccharides, extracted from *Artemisia sphaerocephala* seeds, presenting the same range of Mw and a narrow polydispersity, against human non-small cell lung cancer A549 cells, human hepatocellular carcinoma HepG2cells and human cervical cancer Hela cells. IC_{50} values around 150 µg/mL were obtained in a dose-dependent manner [50]. In a previous study, an OSID (Mw 27 kDa and sulfate content 45 wt%) showed also, at doses ranging from 50 to 200 µg/mL after a time of contact above 100 hours, a significant inhibitory action on cell proliferation of human osteosarcoma, melanoma, lung cancer, and breast cancer cell lines; a slight antiproliferative effect on colon cancer cell lines and no effect on glioblastoma cells whereas heparin did not shown any antiproliferative effect on all cell lines. The antiproliferative effect of this OSID was dose dependent but not associated with a significant effect on cell viability [42].

3.2.2. Effect of OSID4 in combination with doxorubicin

Cell viability was measured to evaluate the effect of OSID4 compared to heparin (100 µg/mL) in combination with increasing concentrations of doxorubicin (from 0.1 ng to 10

µg/mL), a chemotherapy drug. The results obtained for 2 cell lines, after 5 days of treatment, were presented in Fig. 5. For human osteosarcoma cells, the effect of doxorubicin alone (control) showed practically a complete inhibition of cell viability, for a concentration above 1,000 ng/mL (Fig. 5A). At 100 µg/mL of OSID4 alone, 30 % inhibition of cell viability was observed compared to control. In combination with doxorubicin at 100 ng/mL, a greater inhibitory effect of OSID4 was observed, compared to doxorubicin alone, with 50% inhibition of cell viability (yellow bars). This additive inhibitory effect was not noticed when heparin was used with doxorubicin. Indeed, in contrast to OSID4, heparin displayed a weak stimulating effect alone or combined with doxorubicin. The same results were obtained for human non-small cell lung cancer cell line (data not shown). In contrast to OSID4, OSID1 combined with doxorubicin did not show any additional effect compared to single agent (Fig. S4). For human colon cancer (Fig. 5B), doxorubicin could not totally inhibit cell viability even at high doses (above 1,000 ng/mL), same inhibition profile was obtained when heparin was used, showing that heparin did not present any effect on this cell line. On the opposite, OSID4 alone had an inhibitory effect of 40% and in combination with doxorubicin, an additive effect was observed giving an inhibition rate about 50 %, even at low doses of doxorubicin (below 100 ng/mL). Both OSID1 and OSID4 did not show any additive effect combined with doxorubicin in A375 human melanoma cells (Fig. S4B).

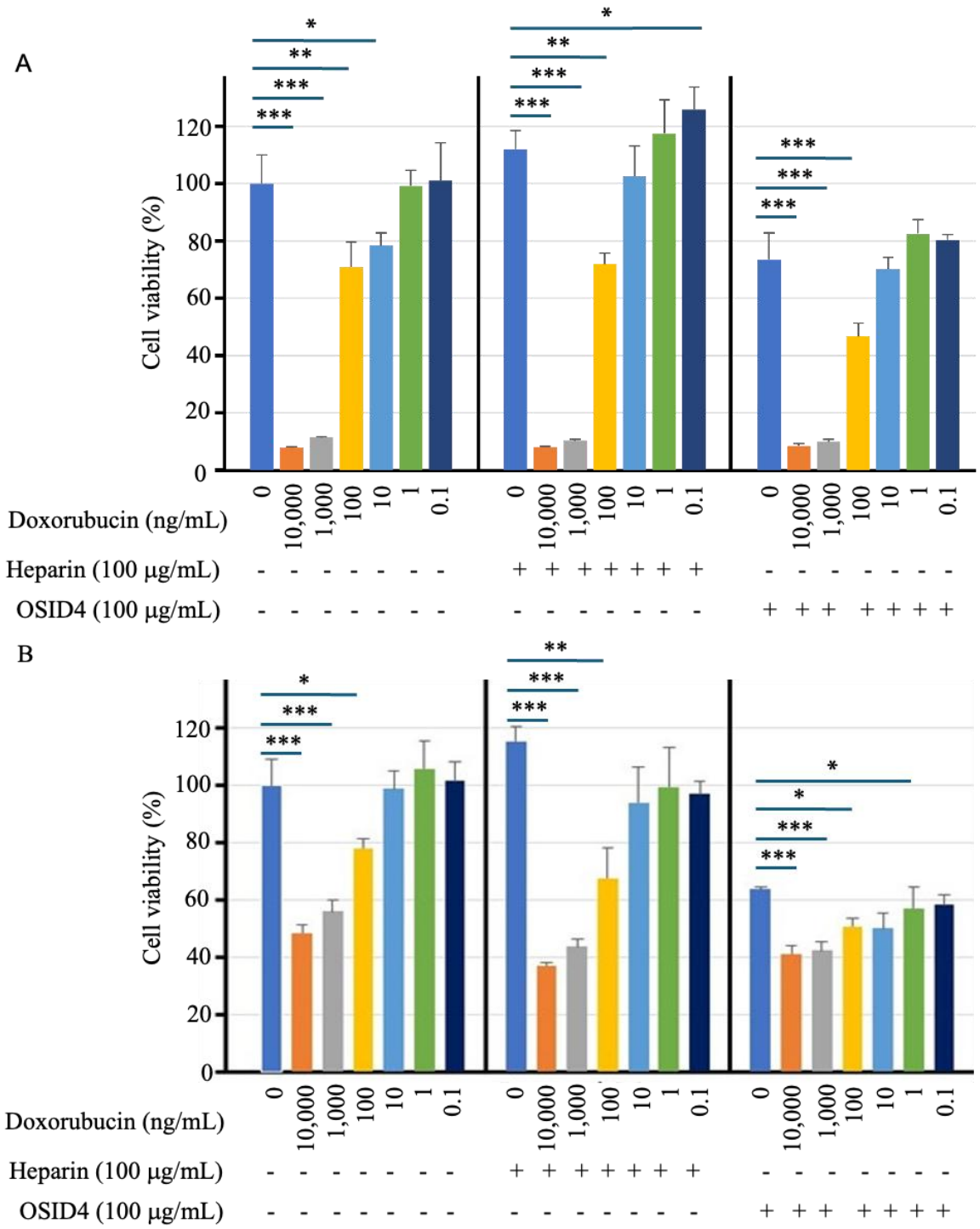

Fig. 5. Effect of OSID4 and heparin combined with doxorubicin. (A) Human MNNG-HOS osteosarcoma cells. (B) $CaCO_2$ colon cancer cells. Cells (n=3,000) were cultured in the presence or the absence of 100 µg/mL of OSID or heparin combined with increased concentrations of doxorubicin. After 96 hours of culture, cell viability was measured by MTT assay. *p< 0.05; **p<0.01; ***p<0.001.

According to the different cancer cell lines used, the effect of doxorubicin as well as OSID4 on cell viability was different although not demonstrating any drug interaction of OSID4 in combination with doxorubicin. These results allow to assume a low probability of unwanted effect with the view that OSID4 would be used as an adjunct to chemotherapy. The development of natural polysaccharides to improve efficacy of chemotherapy is a promising approach since they display antitumor activity with a low toxicity.

Recently, a synergistic inhibitory effect of cisplatin (a chemotherapy drug) and a natural polysaccharide obtained from *Astragalus membranaceus* on an ovarian cancer cell line (SKOV3) treated at 24, 48 and 72 hours was described. The polysaccharide enhanced the sensitivity of cancer cells to the chemotherapeutic drug. The viability of cancer cells was inhibited in a time- and dose-dependent manner [51]. Similarly, a recent study using a natural polysaccharide from *Ganoderma lucidum* in combination with docetaxel (a chemotherapy drug) and the flumatide (anti-androgen drug used to treat prostate cancer) showed that the polysaccharide could synergistically increase the effect of both drugs on the sensitivity of prostate cancer cell lines [52].

3.3. In vivo effects of OSID4 on different cancer cell lines

3.3.1. OSID4 slowed down the progression of lung carcinoma and melanoma in immunocompetent mouse models

Based on the noticed *in vitro* effect of two OSIDs, their therapeutic potential in murine models of lung cancer and melanoma were then assessed (Fig. 6). OSID1 or OSID4, injected subcutaneously at a dose of 10 mg/kg once a day and 5 times a week, significantly slowed down the tumor growth in both studied models compared to the vehicle. Interestingly, in the two tumor-bearing mouse models, no apparent toxicity and no impact on animal weight were noticed. In addition, OSID4 was more efficient to inhibit the tumor progression than OSID1 both in lung cancer and melanoma models. After 25 days of treatment, the tumor progression

in CMT167 lung cancer model was reduced by 55% in the OSID4 treated group compared to the control (Fig. 6A). Similarly, 50% inhibition of tumor growth rate was obtained in B16-F10 melanoma model after 20 days of OSID4 treatment, compared to the control group. A delay of tumor initiation was clearly observed in melanoma-bearing mice treated with OSID4 (Fig. 6B). These results demonstrated that OSID4 had a significant effect on the primary tumor development for both lung carcinoma and melanoma.

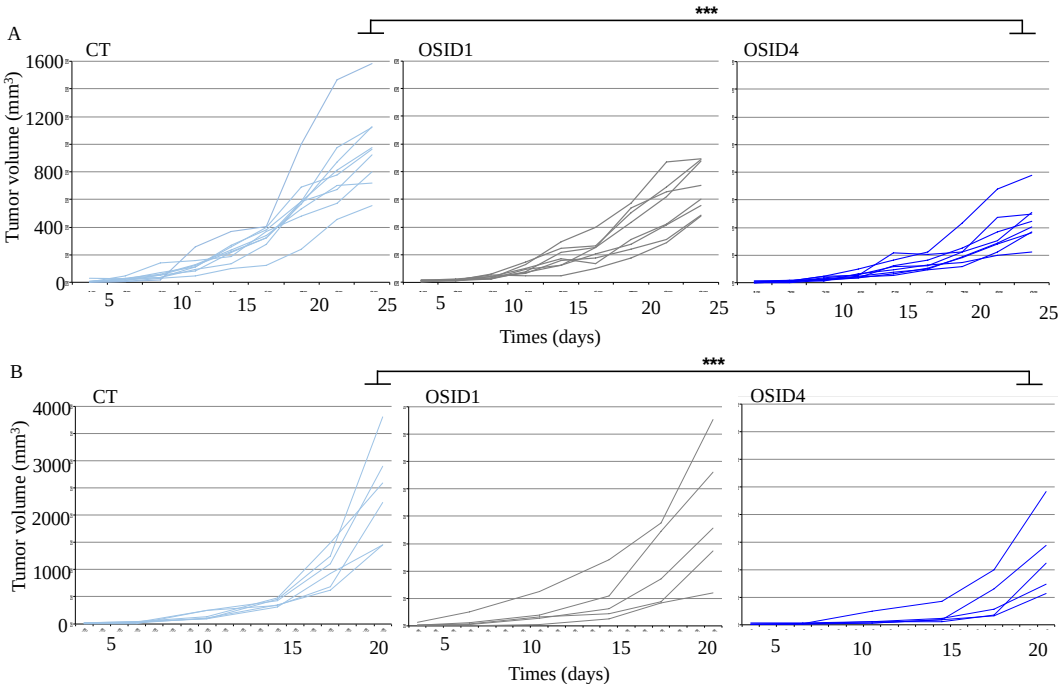

Fig. 6. OSIDs significantly slowed down progression of lung cancer and melanoma in immune competent models. Tumor-bearing immunocompetent mouse model initiated by s.c inoculation of (A) mouse CMT167 lung carcinoma cells (n = 8-9 mice per group) and (B) mouse B16-F10 melanoma cells (n = 5-6 mice per group). Mice were treated 5 times a week at 10 mg/kg of OSID1 or OSID4 by subcutaneous route from 3 days post cell inoculation. Tumor volumes were manually measured twice a week by using a caliper. CT: control group corresponding to mice treated with NaCl as vehicle. ***p<0.001.

Numerous studies reported the antitumoral effect of natural polysaccharides. An important group was constituted by unsulfated polysaccharides rich in neutral monosaccharides, extracted from plants and mushrooms and used in Chinese traditional medicine. Their antitumor effect was monitored in tumor allograft syngeneic mouse models (H22 cell line) and they were administered by gavage before and during treatment, especially for the HMW

polysaccharides (>10^6 Da), once a day at doses above 100 mg/kg [53, 54]. From these studies, inhibition rates were below 50%. In another study, a HMW polysaccharide composed of neutral monosaccharides (mainly mannose, glucose and galactose) could suppress tumor growth with a tumor inhibition rate close to 50% at a dose of 100 mg/kg in S180 mouse sarcoma tumor-bearing mice [55]. For naturally sulfated polysaccharide extracted from macroalgae, such as fucoidan, their antitumor effects have been extensively studied for more than 30 years [25]. Sulfated GAGs such as heparins and also heparin analogs were described for their ability to interfere with cancer progression [10, 16, 56]. A HMW chemically sulfated bacterial polysaccharide (capsular polysaccharide from *E. coli* K5), with a low anticoagulant activity, was effective to reduce tumor burden in bone in a mouse model of breast bone metastasis at a dose of 5 mg/kg administered intravenously daily (after cell inoculation) for 4 weeks per treatment course [57].

3.3.2. OSID4 inhibited the development of human lung cancer in an immunodeficient mouse model

After injection of human non-small cell lung cancer A549 cells, immunodeficient mice were treated for 6 weeks by OSID4 or doxorubicin alone or OSID4 combined with doxorubicin. Tumor size and weight of each mouse were monitored regularly during 42 days (Fig. 7). Interestingly, individual treatment with doxorubicin ($P<0.001$) and OSID4 ($P<0001$) resulted in a potent reduction of tumor volume compared to control group. OSID4 exhibited similar antitumor activity when compared to doxorubicin in this cancer model. The very significant effect of OSID4 on human lung carcinoma tumor progression did not allow to show any significant additive effect of the combined treatment (Fig. 7A). However, the combined treatment did not exhibit any critical toxicity in treated mice. The monitoring of mouse body weight did not reveal any side effect of doxorubicin, OSID4, and combination treatment thereof (Fig. 7B).

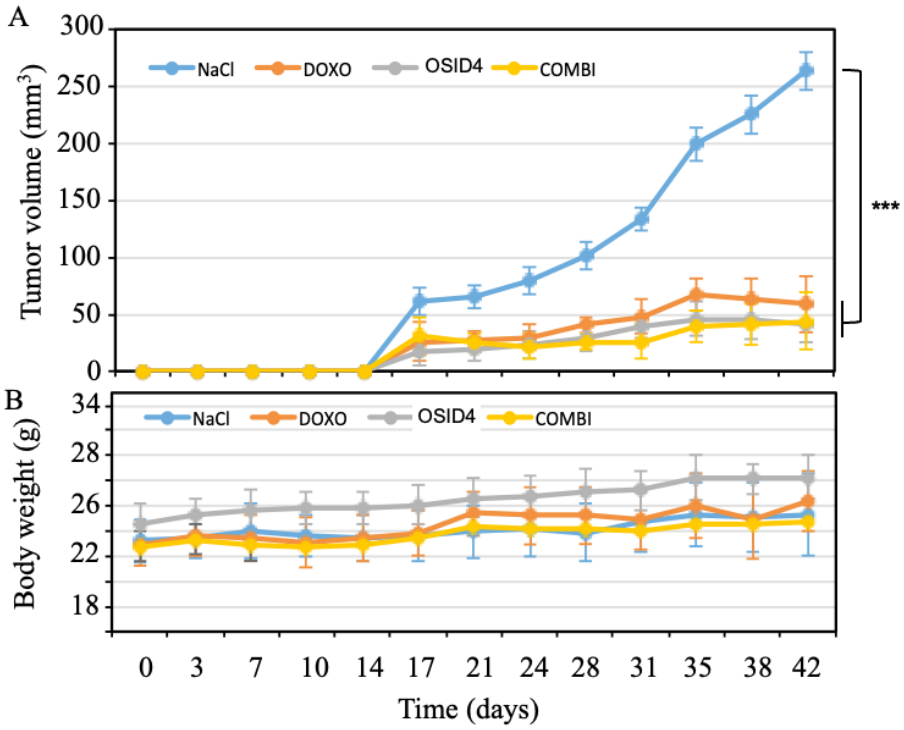

Fig. 7. *In vivo* effect of OSID4 in a tumor-bearing immunodeficient mouse model of human lung cancer, alone or combined with doxorubicin. (A) Tumor volume follow-up after 10^6 A549 human lung carcinoma cell inoculation. OSID4 was injected 5 times a week at 4 mg/kg by subcutaneous route from 3 days post cell inoculation; doxorubicin was injected 3 consecutive days at 3 mg/kg by intravenous route from 3 days post cell inoculation. Tumor volumes were manually measured twice a week by using a caliper. (B) Corresponding body weight of treated mice. N= 6 mice per group. ***p<0.001.

After *in vitro* screening on human cancer cell lines, ectopic tumor xenograft model is considered as a good *in vivo* model for preclinical assessment of an anticancer drug candidate, because the same human cancer cells are used [58]. Moreover even if some components of immune system are missing, some cells are relatively intact (e.g. dendritic cells, B cells, granulocytes) with a compensatory increase in both natural killer cell and tumoricidal macrophage activities [59]. There are very few studies relating to the antitumor properties of polysaccharides combined with doxorubicin in xenograft tumor mouse model. A polysaccharide extracted from Chinese herb, injected intraperitoneally at the dose of 50 mg/kg with doxorubicin (2 mg/kg) every 3 days until day 28, showed in Hep3B xenograft mouse model a tumor growth inhibitory effect higher than doxorubicin alone, the polysaccharide

alone did not exhibit any inhibiting effect. In this study, a synergistical effect was clearly observed suggesting that the *Astragalus* polysaccharide could enhance the sensibility of human hepatocellular carcinoma to doxorubicin and was able to promote doxorubicin efficiency [60]. The same synergistical effect was observed in allograft tumor mouse model with different polysaccharides and chemotherapeutic agents such as cyclophosphamide [55, 61]. UFH-doxorubicin conjugates, injected by intravenous route (11 mg/kg/3days) for 20 days per treatment course in allograft colorectal CT26 tumor mouse model, were very potent to inhibit tumor volume, whereas UFH or doxorubicin alone had only a weak inhibitory effect [62]. In our present study, even if OSID4 and doxorubicin were not injected by the same administration route and at the same time, a stable interaction between highly negatively charged hydrophilic OSID4 and positively charged doxorubicin could occur promoting the enhanced permeability and retention effect at the tumor site [62]. This interaction could also be the consequence of the synergistic effect observed *in vitro* with the different cancer cell lines. In the present study, OSIDs were firstly assessed in non pre-established tumor models and each compound was administered 3 days post cell inoculation (Fig. 6, 7), these conditions representing a limitation in our study. Based on the high efficacy of OSID4 observed on lung cancer development close to the effects of a conventional chemotherapeutic agent (doxorubicin), it would now justify to assess OSID compounds on pre-established tumor. In addition, all tumor cells were inoculated subcutaneously. It would be interesting to evaluate each OSID in orthotopic models as well as in patient derived xenografts. Indeed, the tumor microenvironment may impact not only the tumor growth but also the drug response and the metastatic process [44, 63].

3.4. OSID4 modulated the transcriptomic profile of A549 human lung cancer cell line

Transcriptomic profile of the A549 human lung adenocarcinoma cell line treated or not with OSIDs was carried out by using NanoString technology (Fig. 8). After 24 hours of

treatment, both compounds OSID1 and OSID4, modulated significantly the transcriptomic profile of lung cancer cells as shown by Heatmap visualization and clustering analysis (Fig. S5). More than 30 genes, under 814 genes analyzed, were significantly modulated in the presence of 100 µg/mL OSID4 (Fig. 8A, B). The bioinformatics analyses (KEGG enrichment) showed that the PI3K-Akt and MAPK signaling pathways, proteoglycan regulation in cancer and cell cycle control are among the most modulated by OSID4 (Fig. 8C, D). When A549 lung cancer cells were treated with 100 µg/mL of OSID1, 25 genes related to the same KEGG enrichment pathways were significantly modulated by OSID1 (Fig. S6) and 14 genes (CD274, PTGS2, ADM, TNFAIP3, IL11, PMAIP, CDK1, HLOX1, ALDH1A3, MSH2, β4GALNT1, SOS1, TN4, PDGFβ) were similarly modulated by both OSIDs. Overall, these results demonstrated that cancer cells are direct targets of OSIDs which modulate specific gene profiles.

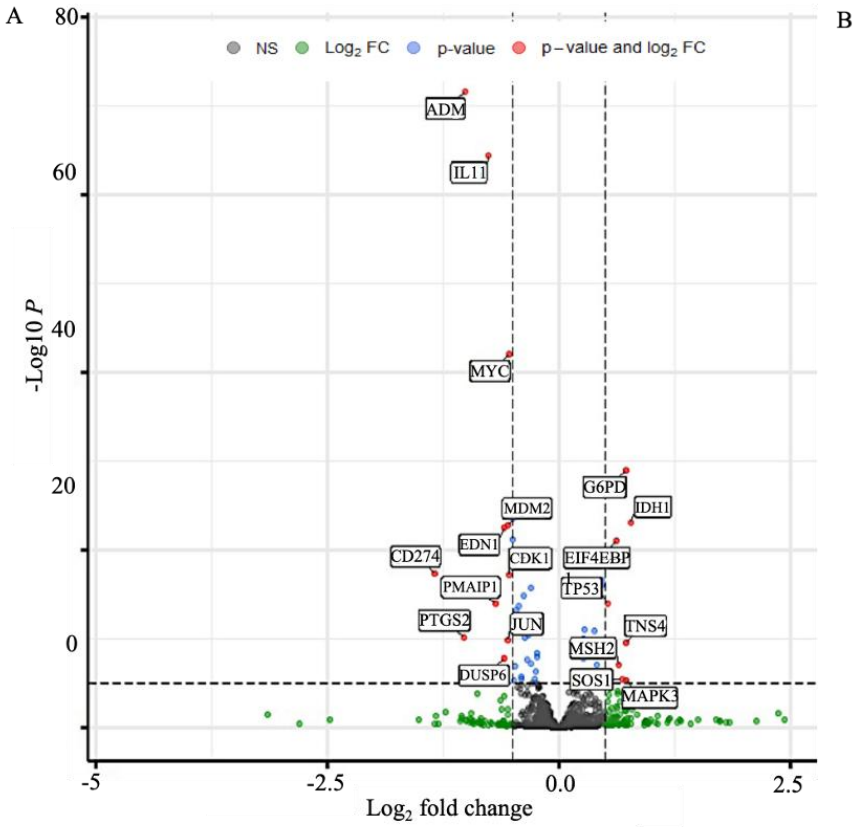

Genes	Log_2 Fold change
CD274	-1.43
PTGS2	-1.13
ADM	-1.03
TNFAIP3	-1.08
IL11	-0.77
PMAIP1	-0.71
BRIP1	-0.71
DUSP6	-0.62
CDCA5	-0.65
EDN1	-0.59
JUN	-0.57
MDM2	-0.56
CDK1	-0.55
MYC	-0.54
TP53	+0.52
CDH1	+0.57
RFC4	+0.57
EIF4BP1	+0.62
HMOX1	+0.63
ALDH1A3	+0.67
MSH2	+0.68
SOS1	+0.73
G6PD	+0.75
TNS4	+0.75
β4GALNT1	+0.77
IDH1	+0.78
PCLAF	+0.79
MAPK3	+0.80
PDGFβ	+0.90
BRCA1	+0.92
CXXC5	+1.1

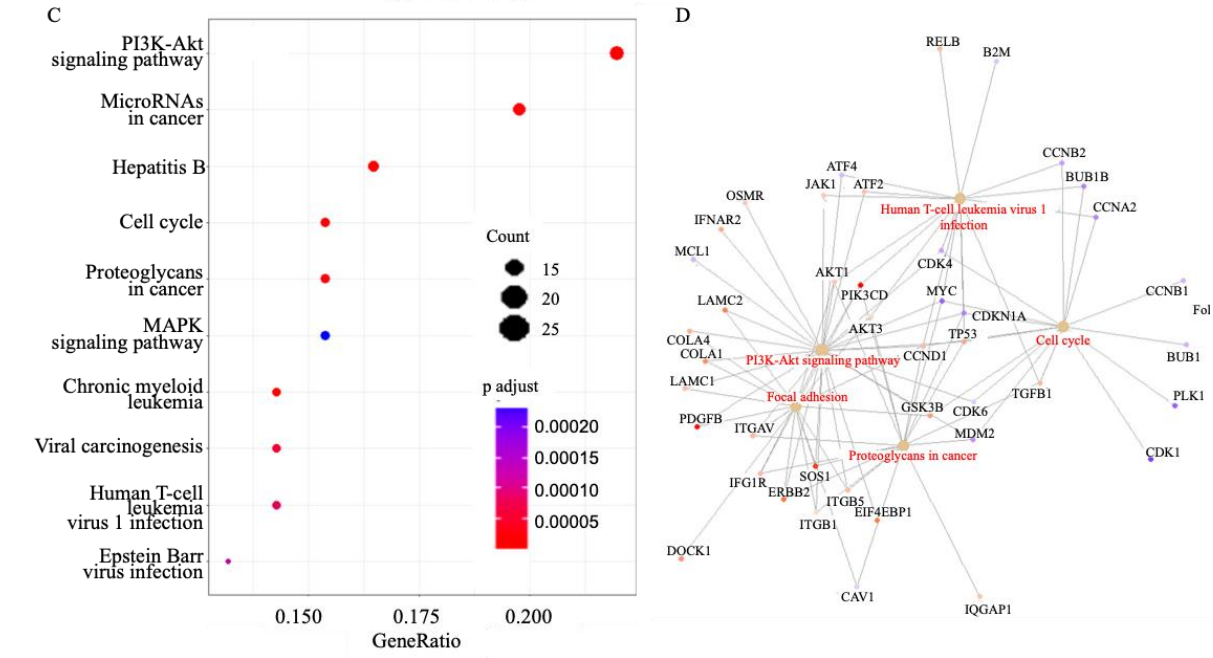

Fig. 8. OSID4 modulated the transcriptomic profile of human lung adenocarcinoma A549 cells. A549 cells were treated or not with 100 µg/mL of OSID4 for 24 hours before RNA extraction. 814 genes were analyzed by using the NH_Hs_TumorSig_v1.0 panel provided by NanoString™. (A) Transcriptomic signature obtained by Nanostring™, comparing A549 cells treated with vehicule or OSID4 for 24 hours. (B) Main genes significantly up or down regulated by OSID4 treatment. (C) Functional predictive analysis of gene clusters modulated by

OSID4. KECG term enrichment analysis of cellular components, biological processes and molecular functions were performed on each gene cluster identified. The size of colored circles is related to the number of genes identified. The color panel corresponds to the variation of the statistical significance. (D) Gene networks related to the main functional pathways regulated. The experiments were conducted in triplicate.

The antitumoral effect of OSID4 observed may be explained by various complementary mechanisms. In a previous study, the regulation of expression of matrix metalloproteinases and their inhibitors by OSID1 in osteosarcoma cells was demonstrated, possibly through modulation of the kinetic of tumor growth and the remodeling of local environment (e.g. extracellular matrix, angiogenesis) [35]. More recently, another OSID (8 kDa and 45 wt% sulfate) tested in a mucopolysaccharidosis IIIA cell line model was shown to prevent heparan sulfate degradation by inhibiting heparanase activity [64]. Heparanase plays important enzymatic and non-enzymatic functions and could contribute to the tumor progression [65]. The regulation of local protease activities by OSIDs, confirmed by the KEGG enrichment pathways analysis (proteoglycans in cancer, focal adhesion), may explain the significant effect observed in the presented cancer models. Rojiani et al. [66] observed a functional relationship between TIMP-1 overexpression in lung cancer and disease progression that strengthens the role of protease regulation in cancer. The functional regulation of MAPK, PI3K-Akt and cell cycle expressed by cancer cells that control the proliferation of cancer cells may complete the potential impact of OSIDs on the local microenvironment. Heparins and heparin mimetics may have immune functions and are functionally based at the cross road of the coagulation and inflammation [67]. Numerous growth factors contain a heparin-binding domain leading to their interactions with polysaccharides. Such interactions exacerbate or repress their biological activities that may explained the potential impact of OSIDs on local microenvironment, immune and cancer cells [68-71]. The interactions between growth factors and integrins expressed at membrane of cancer cells can lead to altered control of mitogenic function of growth factors [72]. In addition by inhibiting the coagulation cascade and

reducing thromboembolic events, polysaccharides could include direct effect of lymphoid organs [73]. VTE became progressively the second-leading cause of death in cancer patients [8]. Their incidence estimated at around 4-20% of cancer depends on the cancer types with a higher risk for lung, pancreas and stomach cancers [7]. In this context, both anti-inflammatory and anticancer activities of anticoagulant drugs are of major interest [74]. All biological properties described for the OSIDs indicate that these derivatives can be considered as heparin analogs and should present advantageous effects for cancer treatment.

3.5. Pharmacokinetic studies

Pharmacokinetic data are essential to enable clinical development of a drug candidate. A study to obtain pharmacokinetic data on OSID4 was then carried out. OSID4 was detectable and quantifiable with good linearity in plasma. After intravenous (iv) injection of 10 mg/kg of OSID4 in male mice, blood was collected at different times and the concentration of OSID4 in mouse plasma was determined (Fig. 9A). Like heparin, dextran sulfate and other heparinoids, OSID4 was found to be rapidly eliminated (less than 4 hours) from the body, possibly due to its high solubility. OSID4 exhibited an anticoagulant activity detectable in plasma. In agreement with the biochemical evaluation, OSID4 anticoagulant activity (corresponding to its concentration in plasma) was no longer detectable after 4 hours following iv injection (Fig. 9C).

A pharmacokinetic study was also conducted after subcutaneous (sc) injection of OSID4 at a dose of 30 mg/kg. The concentration of OSID4 in the plasma was evaluated at the different time points (Fig. 9B). Starting at time point 30 minutes, OSID4 concentration in the plasma increased to reach a maximum at 90 minutes. Then, OSID4 concentration decreased to reach, at 1440 minutes (24 hours), the concentration observed in the control group suggesting its complete elimination from blood. Evaluation of anticoagulant activity also allowed possible

the monitoring and quantification of OSID4, giving an almost identical profile (Fig. 9D) as observed following iv injection.

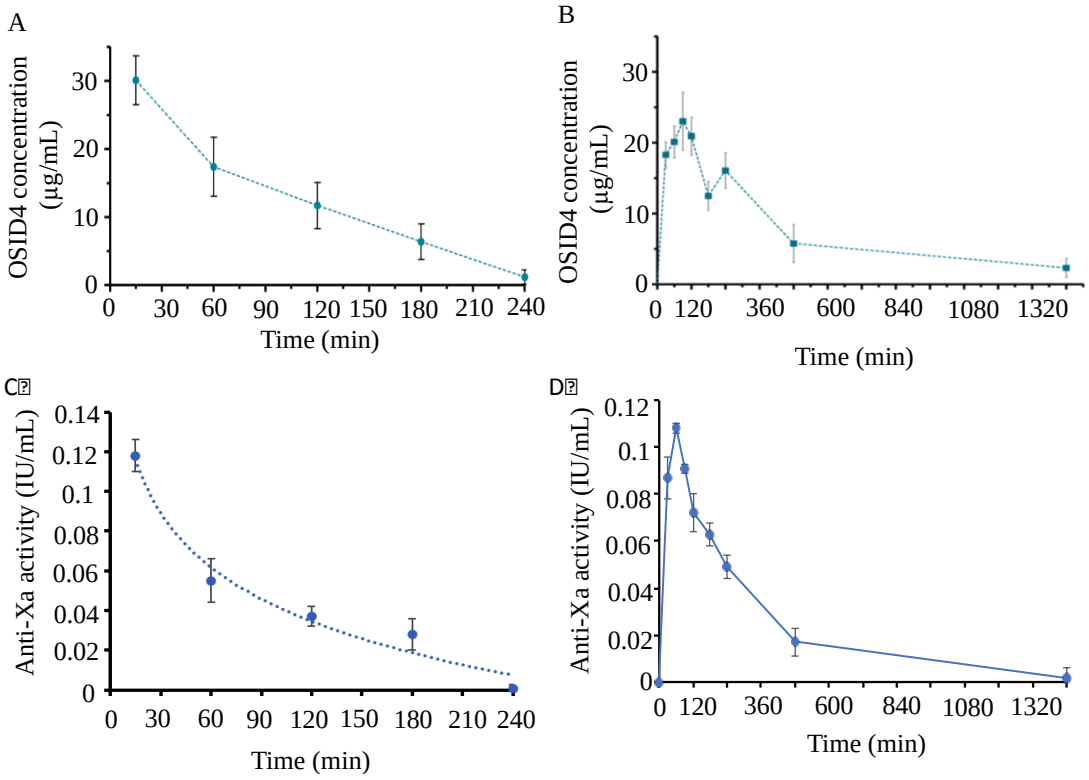

Fig. 9. Pharmacokinetic parameters of OSID4 in mice. Kinetic of plasma concentration of OSID4 after (A) iv injection of 10 mg/kg and (B) sc injection of 30 mg/kg. Anticoagulant activity of OSID4 determined by the follow up of anti-Xa activity after (C) iv injection of 10 mg/kg and (D) sc injection of 30 mg/kg.

The pharmacokinetic parameters of OSID4 were calculated for the two different modes of injection tested (iv and sc) and are presented in Table 2. For the two modes of administration, the maximum concentration (Cmax) of OSID4 in plasma was determined to be 32.8 µg/mL and 30.1 µg/mL, respectively. OSID4 was found to quickly reach the Cmax value and was eliminated with a short half-life. These results indicated that OSID4 had a poor tissue distribution and that its clearance could explain the poor extraction yields at longer times after its administration. Moreover, OSID4 exhibited a high solubility with a high affinity for plasma proteins, which could justify its high bioavailability after sc administration in mice. OSID4 showed similar pharmacokinetic parameters to LMW heparin and therefore renal elimination should be expected as previously observed for LMW heparin [75]. As shown in

the pharmacokinetic study, OSID4 had a moderate anti-Xa activity (below 0.12 IU/mL) at a dose (30 mg/kg sc) higher than those showing a strong tumor volume reduction (10 and 4 mg/kg sc). A low anticoagulant heparin after sc injection at a dose of 20 mg/kg and with a maximum plasma anti-Xa activity of 3 IU/mL did not provoke bleeding [75].

Table 2. Mean pharmacokinetic parameters of OSID4 following its intravenous (iv) or subcutaneous (sc) administration in mice.

Administration pathway and dose	iv 10 mg/kg	sc 30 mg/kg
Ke (μg/mL/h)	0.25 ± 0.13	0.11 ± 0.04
Cmax (μg/mL)	32.8 ± 1.7	30.1 ± 0.9
Tmax (h)	-	1.5 ± 0.5
T1/2 (h)	2.69 ± 1.06	6.65 ± 2.30
AUC (μg.h/mL)	45.3 ±16.2	143.6 ± 48.5
AUMC (μg.h/mL)	2,549 ± 1,331.8	35,945.3 ± 17,043.8
CL (L/h/kg)	0.24 ± 0.09	0.23 ± 0.08
Vd (L/kg)	0.88 ± 0.28	2.00 ± 0.05
MRT (h)	0.89 ± 0.18	4.03 ± 0.66
F (%)	-	105.6 ± 2.6

Ke: Elimination constant rate. Cmax: Maximun drug concentration. Tmax: Time to reach maximum concentration. T1/2: Half-life. AUC: Area under the curve. AUMC: Area under the first moment curve. CL: Clearance. Vd: volume of distribution. MRT: AUMC/AUC Mean resident time. F: subcutaneous bioavailability.

3.6. Toxicological study

The toxicity studies conducted on OSID1 and OSID4, using a mouse model demonstrated that both polysaccharides showed no toxicity at doses of 10 and 30 mg/kg. Histopathological analyses confirmed these observations. No hemorrhagic effect was detected and few side effects such as diarrhea and piloerection were observed at 100 mg/kg. At this very high doses (100 mg/kg), OSID1 caused the death of 2 male mice, one on the 5^{th} day and one on the 6^{th} day of the study (group of 8 mice). However, no mortality was observed with OSID4 even at

613 the very high dose of 100 mg/kg. Overall, these data demonstrated that OSIDs were well
614 tolerated and did not induce any deleterious side effects when administrated by iv or sc route
615 in mice. These results were favorable enough to warrant the use of OSIDs for prolonged
616 thromboprophylaxis after cancer surgery in cancer patients at high risk of venous
617 thromboembolism. In contrast to heparins, OSIDs should prevent any risk of bleeding and
618 should be safe and effective at the doses at which they inhibit tumor growth [8, 76].

619 In the present work, the method of production used leads to bacterial EPS derivatives with
620 controlled size and sulfation rate. These compounds were shown to be active against a range
621 of human and mouse cancer cell lines using highly sensitive *in vitro* real-time techniques such
622 as impedance monitoring (xCELLigence technology). The activities of these EPS derivatives
623 were confirmed by transcriptomic approaches (Nanostring^{TM} approach without DNA
624 amplification step), which allowed to identify several modulated functional pathways.
625 Immunocompetent and immunodeficient mouse models demonstrated the anti-tumor activities
626 of these compounds, with no toxicity observed. Among these EPS derivatives, OSID4 (60
627 kDa, 40 wt% sulfate) emerged as a lead with a dual spectrum of biological activities:
628 anticoagulant and anticancer. OSID4 thus offers therapeutic value in oncological entities
629 associated with a risk of thromboembolic events.

630 **4. Conclusion**

631 OSIDs are oversulfated LMW bacterial EPS derivatives, with a homogenous structure,
632 from non-animal origin and produced by a highly reproducible biotechnological process. Our
633 study showed that OSID4 candidate (60 kDa, 40 wt% sulfate) presents a weak anticoagulant
634 activity, as observed in the pharmacokinetic study, combined with a direct inhibitory effect on
635 cell viability, cell proliferation and also on tumor growth for a large series of human and
636 murine cancer cell lines in both *in vitro* and *in vivo* models, in contrast to UFH and LMWH.
637 Indeed in tumor-bearing immunodeficient mouse model of human lung cancer, OSID4

exhibited antitumor activity comparable to that of doxorubicin, a chemotherapy drug. As well described for some heparins and GAG-mimetics, various mechanisms, highly dependent of the cancer type, can be involved to influence the cancer progression. In A549 human lung cancer cell line, PI3K-Akt, proteoglycans, miRNA and cell cycle regulation are the main molecular pathways regulated by OSID4 indicating a functional impact of OSID4 on cancer cell survival, growth, proliferation and cell adhesion associating an epigenetic regulation, respectively. Pharmacokinetic and toxicity data indicate that OSID4 is readily compatible with drug development in cancerology. Moreover, its weak anticoagulant activity did not induce any bleeding events in treated mice and toxic responses. Interestingly, combined therapies are frequently used in cancer treatments and here the association of chemotherapy and OSID4 did not show any deleterious side effects in the assessed murine models. With a controllable moderate anticoagulant activity, pharmacokinetic parameters comparable to heparins and a notable *in vivo* anticancer activity, OSID4 constitutes a promising agent for the treatment of cancer patients with high incidence of thrombosis. The absence of toxicity confirms this potential. The data obtained in this study encourage the consideration of OSID4 as a new natural anticancer agent that could be used in combinatorial therapies to treat patients at high risk of thromboembolic events undergoing chemotherapy or prior to cancer surgery. In combination with chemotherapy, immunotherapy or targeted therapy, OSID4 should reduce serious side effects such as bleeding and improve quality of life. Overall, the present study identified the therapeutic value of OSID4 in oncologic entities associated with a risk of thromboembolic events (e.g. lung, pancreatic, stomach cancer or glioblastoma).

Declarations of competing interest

The authors declare no conflict of interest.

Acknowledgement

The authors would like to thank SATT Ouest Valorisation for Engineer funding (A.A.). Financial supports were provided by SATT Ouest Valorisation and Ifremer.

CRediT authorship contribution statement

Dominique Heymann: Conceptualization, Investigation, Funding acquisition, Writing – Original Draft, Writing – Review & Editing; **Javier Muñoz-Garcia** and **Antoine Babuty**: Methodology, Investigation, Formal analysis, Validation, Writing – Review & Editing ; **Antoine Audéon**: Methodology, Investigation, Formal analysis and Validation; **Dulce Papy-Garcia** and **Sandrine Chantepie:** Methodology, Investigation, Formal analysis, Writing, Validation; **Agata Zykwinska:** Conceptualization, Investigation, Writing – Review & Editing ; **Corinne Sinquin**: Methodology, Investigation, Formal analysis, Writing – Review & Editing; **Sylvia Colliec-Jouault**: Conceptualization, Investigation, Funding acquisition, Writing – Original Draft, Writing – Review & Editing.

Appendix A. Supplementary data

Data availability: Data will be made available on request.

References

[1] C. Mattiuzzi, G. Lippi, Current Cancer Epidemiology, Journal of Epidemiology and Global Health, 9 (2019), 217-222, https://doi.org/10.2991/jegh.k.191008.001.

[2] M. Schlander, W. van Harten, V.P. Retèl, P.D. Pham, J.M. Vancoppenolle, J. Ubels, O.S. López, C. Quirland, F. Maza, E. Aas, B. Crusius, A. Escobedo, N. Franzen, J. Fuentes-Cid, D. Hernandez, K. Hernandez-Villafuerte, I. Kirac, A. Paty, T. Philip, S. Smeland, R. Sullivan, E. Vanni, S. Varga, T. Vermeulin, R.D. Eckford, The socioeconomic impact of cancer on patients and their relatives: Organisation of European Cancer Institutes task force consensus recommendations on conceptual framework, taxonomy, and research directions, Lancet Oncology, 25 (2024) e152-e16, https://doi.org/10.1016/S1470-2045(23)00636-8.

[3] Y. Pu, L. Li, H.N. Peng, L.X. Liu, D. Heymann, C. Robert, F. Vallette, S.S. Shen, Drug-tolerant persister cells in cancer: the cutting edges and future directions, Nature Reviews Clinical Oncology, 20 (2023) 799-813, https://doi.org/10.1038/s41571-023-00815-5.

[4] S.U. Khan, K. Fatima, S. Aisha, F. Malik, Unveiling the mechanisms and challenges of cancer drug resistance, Cell Communication and Signaling, 22 (2024), https://doi.org/10.1186/s12964-023-01302-1.

[5] V. Schirrmacher, From chemotherapy to biological therapy: A review of novel concepts to reduce the side effects of systemic cancer treatment (Review), Int. J. Oncol., 54 (2019) 407-419, https://doi.org/10.3892/ijo.2018.4661.

[6] D.T. Debela, S.G. Muzazu, K.D. Heraro, M.T. Ndalama, B.W. Mesele, D.C. Haile, S.K. Kitui, T. Manyazewal, New approaches and procedures for cancer treatment: Current perspectives, SAGE Open Medicine, 9 (2021) 20503121211034366, https://doi.org/10.1177/20503121211034366.

[7] N.B.A. Razak, G. Jones, M. Bhandari, M.C. Berndt, P. Metharom, Cancer-Associated Thrombosis: An Overview of Mechanisms, Risk Factors, and Treatment, Cancers, 10 (2018), https://doi.org/10.3390/cancers10100380.

[8] A. Falanga, C. Ay, M. Di Nisio, G. Gerotziafas, L. Jara-Palomares, F. Langer, R. Lecumberri, M. Mandala, A. Maraveyas, I. Pabinger, M. Sinn, K. Syrigos, A. Young, K. Jordan, Venous thromboembolism in cancer patients: ESMO Clinical Practice Guideline☆, Ann. Oncol., 34 (2023) 452-467, https://doi.org/10.1016/j.annonc.2022.12.014.

[9] A.W. Rutjes, E. Porreca, M. Candeloro, E. Valeriani, M. Di Nisio, Primary prophylaxis for venous thromboembolism in ambulatory cancer patients receiving chemotherapy, The Cochrane database of systematic reviews, 12 (2020) Cd008500, https://doi.org/10.1002/14651858.CD008500.pub5.

[10] R. Wieboldt, H. Läubli, Glycosaminoglycans in cancer therapy, American Journal of Physiology-Cell Physiology, 322 (2022) C1187-C1200, https://doi.org/10.1152/ajpcell.00063.2022.

[11] J.L. Stevenson, A. Varki, L. Borsig, Heparin attenuates metastasis mainly due to inhibition of P- and L-selectin, but non-anticoagulant heparins can have additional effects, Thrombosis Research, 120 (2007) S107-S111, https://doi.org/10.1016/s0049-3848(07)70138-x.

[12] C.R. Velasco, S. Colliec-Jouault, F. Redini, D. Heymann, M. Padrines, Proteoglycans on bone tumor development, Drug Discov. Today, 15 (2010) 553-560, https://doi.org/10.1016/j.drudis.2010.05.009.

[13] A. Badri, A. Williams, R.J. Linhardt, M.A.G. Koffas, The road to animal-free glycosaminoglycan production: current efforts and bottlenecks, Curr. Opin. Biotechnol., 53 (2018) 85-92, https://doi.org/10.1016/j.copbio.2017.12.018.

[14] R. Sasisekharan, Z. Shriver, G. Venkataraman, U. Narayanasami, Roles of heparan-sulphate glycosaminoglycans in cancer, Nature Reviews Cancer, 2 (2002) 521-528, https://doi.org/10.1038/nrc842.

[15] V. Bobek, J. Kovarík, Antitumor and antimetastatic effect of warfarin and heparins, Biomed. Pharmacother., 58 (2004) 213-219, https://doi.org/10.1016/j.biopha.2003.11.007.

[16] C. Lanzi, G. Cassinelli, Heparan Sulfate Mimetics in Cancer Therapy: The Challenge to Define Structural Determinants and the Relevance of Targets for Optimal Activity, Molecules, 23 (2018), https://doi.org/10.3390/molecules23112915.

[17] K. Dredge, T.V. Brennan, E. Hammond, J.D. Lickliter, L.W. Lin, D. Bampton, P. Handley, F. Lankesheer, G. Morrish, Y.P. Yang, M.P. Brown, M. Millward, A Phase I study of the novel immunomodulatory agent PG545 (pixatimod) in subjects with advanced solid tumours, Br. J. Cancer, 118 (2018) 1035-1041, https://doi.org/10.1038/s41416-018-0006-0.
[18] A. Eftekhari, C. Kryschi, D. Pamies, S. Gulec, E. Ahmadian, D. Janas, S. Davaran, R. Khalilov, Natural and synthetic nanovectors for cancer therapy, Nanotheranostics, 7 (2023) 236-257, https://doi.org/10.7150/ntno.77564.
[19] M. Lakhdar, CALOTROPIS PROCERA (AIT) R. BR, A VALUABLE MEDICINE PLANT: A REVIEW, Advances in Biology & Earth Sciences, 8 (2023).
[20] J. Valcarcel, R. Novoa-Carballal, R.I. Pérez-Martín, R.L. Reis, J.A. Vázquez, Glycosaminoglycans from marine sources as therapeutic agents, Biotechnol. Adv., 35 (2017) 711-725, https://doi.org/10.1016/j.biotechadv.2017.07.008.
[21] R. Guo, M. Chen, Y. Ding, P. Yang, M. Wang, H. Zhang, Y. He, H. Ma, Polysaccharides as Potential Anti-tumor Biomacromolecules —A Review, Frontiers in Nutrition, 9 (2022), https://doi.org/10.3389/fnut.2022.838179.
[22] H.-B. Park, S.-M. Lim, J. Hwang, W. Zhang, S. You, J.-O. Jin, Cancer immunotherapy using a polysaccharide from Codium fragile in a murine model, OncoImmunology, 9 (2020) 1772663, https://doi.org/10.1080/2162402X.2020.1772663.
[23] K.O.A.L. Lins, D.P. Bezerra, A.P.N.N. Alves, N.M.N. Alencar, M.W. Lima, V.M. Torres, W.R.L. Farias, C. Pessoa, M.O. de Moraes, L.V. Costa-Lotufo, Antitumor properties of a sulfated polysaccharide from the red seaweed Champia feldmannii (Diaz-Pifferer), J. Appl. Toxicol., 29 (2009) 20-26, https://doi.org/10.1002/jat.1374.
[24] L.Q. Sun, J.L. Chu, Z.L. Sun, L.H. Chen, Physicochemical properties, immunomodulation and antitumor activities of polysaccharide from Pavlova viridis, Life Sciences, 144 (2016) 156-161, https://doi.org/10.1016/j.lfs.2015.11.013.
[25] H. Yu, Q. Zhang, A.A. Farooqi, J. Wang, Y. Yue, L. Geng, N. Wu, Opportunities and challenges of fucoidan for tumors therapy, Carbohydr. Polym., 324 (2024) 121555, https://doi.org/10.1016/j.carbpol.2023.121555.
[26] S. Zhang, Y. Li, Z. Li, W. Liu, H. Zhang, Y. Ohizumi, A. Nakajima, J. Xu, Y. Guo, Structure, anti-tumor activity, and potential anti-tumor mechanism of a fungus polysaccharide from Fomes officinalis, Carbohydr. Polym., 295 (2022) 119794, https://doi.org/10.1016/j.carbpol.2022.119794.
[27] P.L. DeAngelis, Glycosaminoglycan polysaccharide biosynthesis and production: today and tomorrow, Applied Microbiology and Biotechnology, 94 (2012) 295-305, https://doi.org/10.1007/s00253-011-3801-6.
[28] D. Cimini, M. De Rosa, C. Schiraldi, Production of glucuronic acid-based polysaccharides by microbial fermentation for biomedical applications, Biotechnology Journal, 7 (2012) 237-250, https://doi.org/10.1002/biot.201100242.
[29] L. Teng, H. Fu, C. Deng, J. Chen, J. Chen, Modulating the SDF-1/CXCL12-induced cancer cell growth and adhesion by sulfated K5 polysaccharides in vitro, Biomedicine & Pharmacotherapy, 73 (2015) 29-34, https://doi.org/10.1016/j.biopha.2015.05.009.
[30] S. Colliec-Jouault, C.D. Bavington, C. Delbarre-Ladrat, Heparin-like entities from marine organisms, Handb. Exp. Pharmacol., 207 (2012) 423-449, https://doi.org/.
[31] J. Schmid, V. Sieber, B. Rehm, Bacterial exopolysaccharides: biosynthesis pathways and engineering strategies, Frontiers in Microbiology, 6 (2015) 496, https://doi.org/10.3389/fmicb.2015.00496.
[32] K. Akoumany, A. Zykwinska, C. Sinquin, L. Marchand, M. Fanuel, D. Ropartz, H. Rogniaux, M. Pipelier, C. Delbarre-Ladrat, S. Colliec-Jouault, Characterization of New Oligosaccharides Obtained by An Enzymatic Cleavage of the Exopolysaccharide Produced by the Deep-Sea Bacterium Alteromonas infernus Using its Cell Extract, Molecules, 24 (2019) 3441, https://doi.org/10.3390/molecules24193441.
[33] O. Roger, N. Kervarec, J. Ratiskol, S. Colliec-Jouault, L. Chevolot, Structural studies of the main exopolysaccharide produced by the deep-sea bacterium Alteromonas infernus, Carbohydr. Res., 339 (2004) 2371-2380, https://doi.org/10.1016/j.carres.2004.07.021.

[34] S. Colliec Jouault, L. Chevolot, D. Helley, J. Ratiskol, A. Bros, C. Sinquin, O. Roger, A.-M. Fischer, Characterization, chemical modifications and in vitro anticoagulant properties of an exopolysaccharide produced by Alteromonas infernus, Biochimica et Biophysica Acta (BBA) - General Subjects, 1528 (2001) 141-151, https://doi.org/10.1016/S0304-4165(01)00185-4.
[35] D. Heymann, C. Ruiz-Velasco, J. Chesneau, J. Ratiskol, C. Sinquin, S. Colliec-Jouault, Anti-Metastatic Properties of a Marine Bacterial Exopolysaccharide-Based Derivative Designed to Mimic Glycosaminoglycans, Molecules, 21 (2016) 309, https://doi.org/10.3390/molecules21030309
[36] R.B. Mokhtari, T.S. Homayouni, N. Baluch, E. Morgatskaya, S. Kumar, B. Das, H. Yeger, Combination therapy in combating cancer, Oncotarget, 8 (2017), https://doi.org/10.18632/oncotarget.16723
[37] J. Guezennec, P. Pignet, Y. Lijour, E. Gentric, J. Ratiskol, S. Colliec-Jouault, Sulfation and depolymerization of a bacterial exopolysaccharide of hydrothermal origin, Carbohydr. Polym., 37 (1998) 19-24, https://doi.org/10.1016/S0144-8617(98)00006-X.
[38] N. Chopin, C. Sinquin, J. Ratiskol, A. Zykwinska, P. Weiss, S. Cérantola, J. Le Bideau, S. Colliec-Jouault, A Direct Sulfation Process of a Marine Polysaccharide in Ionic Liquid, BioMed Research International, 2015 (2015) 508656, https://doi.org/10.1155/2015/508656.
[39] P. Gélébart, S. Cuenot, C. Sinquin, B. Halgand, S. Sourice, C. Le Visage, J. Guicheux, S. Colliec-Jouault, A. Zykwinska, Microgels based on Infernan, a glycosaminoglycan-mimetic bacterial exopolysaccharide, as BMP-2 delivery systems, Carbohydr. Polym., 284 (2022) 119191, https://doi.org/10.1016/j.carbpol.2022.119191.
[40] M.J. Joliat, S. Umeda, B.L. Lyons, M.A. Lynes, L.D. Shultz, Establishment and characterization of a new osteogenic cell line (MOS-J) from a spontaneous C57BL/6J mouse osteosarcoma, In Vivo, 16 (2002) 223-228.
[41] J. van Meerloo, G.J.L. Kaspers, J. Cloos, Cell Sensitivity Assays: The MTT Assay, in: I.A. Cree (Ed.) Cancer Cell Culture: Methods and Protocols, Humana Press, Totowa, NJ, 2011, pp. 237-245, https://doi.org/10.1007/978-1-61779-080-5_20
[42] J. Muñoz-Garcia, M. Mazza, C. Alliot, C. Sinquin, S. Colliec-Jouault, D. Heymann, S. Huclier-Markai, Antiproliferative Properties of Scandium Exopolysaccharide Complexes on Several Cancer Cell Lines, Mar. Drugs, 19 (2021) 174, https://doi.org/10.3390/md19030174
[43] C. Jubelin, J. Muñoz-Garcia, E. Ollivier, D. Cochonneau, F. Vallette, M.F. Heymann, L. Oliver, D. Heymann, Identification of MCM4 and PRKDC as new regulators of osteosarcoma cell dormancy based on 3D cell cultures, Biochimica et biophysica acta. Molecular cell research, 1871 (2024), https://doi.org/119660 10.1016/j.bbamcr.2024.119660.
[44] V.G. Desai, E.H. Herman, C.L. Moland, W.S. Branham, S.M. Lewis, K.J. Davis, N.I. George, T. Lee, S. Kerr, J.C. Fuscoe, Development of doxorubicin-induced chronic cardiotoxicity in the B6C3F1 mouse model, Toxicol. Appl. Pharmacol., 266 (2013) 109-121, https://doi.org/10.1016/j.taap.2012.10.025.
[45] J. Muñoz-Garcia, J.W. Vargas-Franco, B.B.-L. Royer, D. Cochonneau, J. Amiaud, M.-F. Heymann, D. Heymann, F. Lézot, Inhibiting Endothelin Receptors with Macitentan Strengthens the Bone Protective Action of RANKL Inhibition and Reduces Metastatic Dissemination in Osteosarcoma, Cancers, 14 (2022) 1765, https://doi.org/10.1016/10.3390/cancers14071765
[46] I. Barbosa, S. Garcia, V. Barbier-Chassefière, J.P. Caruelle, I. Martelly, D. Papy-García, Improved and simple micro assay for sulfated glycosaminoglycans quantification in biological extracts and its use in skin and muscle tissue studies, Glycobiology, 13 (2003) 647-653, https://doi.org/10.1016/10.1093/glycob/cwg082.
[47] M.B. Huynh, J. Villares, J.E.S. Díaz, S. Christiaans, G. Carpentier, M.O. Ouidja, L. Sissoeff, R. Raisman-Vozari, D. Papy-Garcia, Glycosaminoglycans from aged human hippocampus have altered capacities to regulate trophic factors activities but not Aβ42 peptide toxicity, Neurobiol. Aging, 33 (2012), https://doi.org/10.1016/10.1016/j.neurobiolaging.2011.09.030.
[48] S. Charef, E. Petit, D. Barritault, J. Courty, J.P. Caruelle, Effects on coagulation of a synthetic heparan mimetic given intraperitoneally or orally, Journal of Biomedical Materials Research Part A, 83A (2007), https://doi.org/10.1016/1024-1031 10.1002/jbm.a.31385.
[49] S. Colliec-Jouault, F. Esposito, H. Ledru, C. Sinquin, L. Marchand, A. Fillaudeau, S. Routier, F. Buron, C. Lopin-Bon, S. Cuenot, E. Bedini, A. Zykwinska, Glycosaminoglycan Mimetics

Obtained by Microwave-Assisted Sulfation of Marine Bacterium Sourced Infernan Exopolysaccharide, Biomacromolecules, 24 (2023) 462-470, https://doi.org/10.1016/10.1021/acs.biomac.2c01277.
[50] J. Wang, A. Bao, X. Meng, H. Guo, Y. Zhang, Y. Zhao, W. Kong, J. Liang, J. Yao, J. Zhang, An efficient approach to prepare sulfated polysaccharide and evaluation of anti-tumor activities in vitro, Carbohydr. Polym., 184 (2018) 366-375, https://doi.org/10.1016/j.carbpol.2017.12.065.
[51] C. Li, L. Hong, C. Liu, J. Min, M. Hu, W. Guo, Astragalus polysaccharides increase the sensitivity of SKOV3 cells to cisplatin, Arch. Gynecol. Obstet., 297 (2018) 381-386, https://doi.org/10.1016/10.1007/s00404-017-4580-9.
[52] R. Rahimnia, M.R. Akbari, A.F. Yasseri, D. Taheri, A. Mirzaei, H.A. Ghajar, P.D. Farashah, L.Z. Baghdadabad, S.M.K. Aghamir, The effect of Ganoderma lucidum polysaccharide extract on sensitizing prostate cancer cells to flutamide and docetaxel: an in vitro study, Scientific Reports, 13 (2023) 18940, https://doi.org/10.1016/10.1038/s41598-023-46118-8.
[53] C. Liu, K.-y. Dai, H.-y. Ji, X.-y. Jia, A.-j. Liu, Structural characterization of a low molecular weight Bletilla striata polysaccharide and antitumor activity on H22 tumor-bearing mice, International Journal of Biological Macromolecules, 205 (2022) 553-562, https://doi.org/10.1016/j.ijbiomac.2022.02.073.
[54] X. Tang, J. Huang, H. Xiong, K. Zhang, C. Chen, X. Wei, X. Xu, Q. Xie, R. Huang, Anti-Tumor Effects of the Polysaccharide Isolated from Tarphochlamys Affinis in H22 Tumor-Bearing Mice, Cell. Physiol. Biochem., 39 (2016), https://doi.org/10.1016/1040-1050 10.1159/000447811.
[55] J. Zheng, T. Zhang, J. Fan, Y. Zhuang, L. Sun, Protective effects of a polysaccharide from Boletus aereus on S180 tumor-bearing mice and its structural characteristics, International Journal of Biological Macromolecules, 188 (2021) 1-10, https://doi.org/10.1016/j.ijbiomac.2021.07.191.
[56] N. Afratis, C. Gialeli, D. Nikitovic, T. Tsegenidis, E. Karousou, A.D. Theocharis, M.S. Pavao, G.N. Tzanakakis, N.K. Karamanos, Glycosaminoglycans: key players in cancer cell biology and treatment, FEBS J., 279 (2012) 1177-1197, https://doi.org/10.1016/10.1111/j.1742-4658.2012.08529.x.
[57] S. Pollari, R.S. Käkönen, K.S. Mohammad, J.P. Rissanen, J.M. Halleen, A. Wärri, L. Nissinen, M. Pihlavisto, A. Marjamäki, M. Perälä, T.A. Guise, O. Kallioniemi, S.-M. Käkönen, Heparin-like Polysaccharides Reduce Osteolytic Bone Destruction and Tumor Growth in a Mouse Model of Breast Cancer Bone Metastasis, Mol Cancer Res, 10 (2012) 597-604, https://doi.org/10.1016/10.1158/1541-7786.mcr-11-0482.
[58] J. Jung, Human Tumor Xenograft Models for Preclinical Assessment of Anticancer Drug Development, Toxicological Research, 30 (2014) 1-5, https://doi.org/10.1016/10.5487/TR.2014.30.1.001.
[59] A. Richmond, Y. Su, Mouse xenograft models vs GEM models for human cancer therapeutics, Disease Models & Mechanisms, 1 (2008) 78-82, https://doi.org/10.1016/10.1242/dmm.000976.
[60] M. Li, F. Duan, Z. Pan, X. Liu, W. Lu, C. Liang, Z. Fang, P. Peng, D. Jia, Astragalus Polysaccharide Promotes Doxorubicin-Induced Apoptosis by Reducing O-GlcNAcylation in Hepatocellular Carcinoma, Cells, 12 (2023) 866, https://doi.org/10.3390/cells12060866
[61] M.M. Joseph, S.R. Aravind, S.K. George, S. Varghese, T.T. Sreelekha, A galactomannan polysaccharide from Punica granatum imparts in vitro and in vivo anticancer activity, Carbohydr. Polym., 98 (2013) 1466-1475, https://doi.org/10.1016/j.carbpol.2013.07.023.
[62] J.-H. Lee, S.-B. Yang, J.-H. Lee, H. Lim, S. Lee, T.-B. Kang, J.-H. Lim, Y.J. Kim, J. Park, Doxorubicin covalently conjugated heparin displays anti-cancer activity as a self-assembled nanoparticle with a low-anticoagulant effect, Carbohydr. Polym., 314 (2023) 120930, https://doi.org/10.1016/j.carbpol.2023.120930.
[63] T.G. Grünewald, M. Alonso, S. Avnet, A. Banito, S. Burdach, F. Cidre- Aranaz, G. Di Pompo, M. Distel, H. Dorado- Garcia, J. Garcia- Castro, L. González- González, A.E. Grigoriadis, M. Kasan, C. Koelsche, M. Krumbholz, F. Lecanda, S. Lemma, D.L. Longo, C. Madrigal- Esquivel, Á. Morales- Molina, J. Musa, S. Ohmura, B. Ory, M. Pereira- Silva, F. Perut, R. Rodriguez, C. Seeling, N. Al Shaaili, S. Shaabani, K. Shiavone, S. Sinha, E.M. Tomazou, M. Trautmann, M. Vela, Y.M. Versleijen- Jonkers, J. Visgauss, M. Zalacain, S.J.

Schober, A. Lissat, W.R. English, N. Baldini, D. Heymann, Sarcoma treatment in the era of molecular medicine, EMBO Molecular Medicine, 12 (2020) e11131, https://doi.org/10.15252/emmm.201911131.
[64] N. Veraldi, I.D. Quadri, Y. van de Looij, L.M. Modernell, C. Sinquin, A. Zykwinska, B.B. Tournier, F. Dalonneau, H. Li, J.-P. Li, P. Millet, R. Vives, S. Colliec-Jouault, A. de Agostini, E.F. Sanches, S.V. Sizonenko, Low-molecular weight sulfated marine polysaccharides: Promising molecules to prevent neurodegeneration in mucopolysaccharidosis IIIA?, Carbohydr. Polym., 320 (2023) 121214, https://doi.org/10.1016/j.carbpol.2023.121214.
[65] I. Vlodavsky, Y. Kayal, M. Hilwi, S. Soboh, R.D. Sanderson, N. Ilan, Heparanase—A single protein with multiple enzymatic and nonenzymatic functions, Proteoglycan Research, 1 (2023) e6, https://doi.org/10.1002/pgr2.6.
[66] M.V. Rojiani, S. Ghoshal-Gupta, A. Kutiyanawalla, S. Mathur, A.M. Rojiani, TIMP-1 Overexpression in Lung Carcinoma Enhances Tumor Kinetics and Angiogenesis in Brain Metastasis, J. Neuropathol. Exp. Neurol., 74 (2015) 293-304, https://doi.org/10.1097/nen.0000000000000175.
[67] A.T. Bauer, C. Gorzelanny, C. Gebhardt, K. Pantel, S.W. Schneider, Interplay between coagulation and inflammation in cancer: Limitations and therapeutic opportunities, Cancer Treat. Rev., 102 (2022) 102322, https://doi.org/10.1016/j.ctrv.2021.102322.
[68] S. Matou, S. Colliec-Jouault, I. Galy-Fauroux, J. Ratiskol, C. Sinquin, J. Guezennec, A.-M. Fischer, D. Helley, Effect of an oversulfated exopolysaccharide on angiogenesis induced by fibroblast growth factor-2 or vascular endothelial growth factor *in vitro*, Biochem. Pharmacol., 69 (2005) 751-759, https://doi.org/10.1016/j.bcp.2004.11.021
[69] C. Ruiz Velasco, M. Baud'huin, C. Sinquin, M. Maillasson, D. Heymann, S. Colliec-Jouault, M. Padrines, Effects of a sulfated exopolysaccharide produced by Altermonas infernus on bone biology, Glycobiology, 21 (2011) 781-795, https://doi.org/10.1016/10.1093/glycob/cwr002.
[70] C. Sun, M. Liu, P. Sun, M. Yang, E.A. Yates, Z. Guo, D.G. Fernig, Sulfated polysaccharides interact with fibroblast growth factors and protect from denaturation, FEBS Open Bio, 9 (2019) 1477-1487, https://doi.org/10.1002/2211-5463.12696.
[71] W.W. Ho, M.J. Pittet, D. Fukumura, R.K. Jain, The local microenvironment matters in preclinical basic and translational studies of cancer immunology and immunotherapy, Cancer Cell, 40 (2022) 701-702, https://doi.org/10.1016/j.ccell.2022.05.016.
[72] Y.K. Takada, J. Yu, X. Ye, C.-Y. Wu, B.H. Felding, M. Fujita, Y. Takada, The heparin-binding domain of VEGF165 directly binds to integrin αvβ3 and VEGFR2/KDR D1: a potential mechanism of negative regulation of VEGF165 signaling by αvβ3, Frontiers in Cell and Developmental Biology, 12 (2024), https://doi.org/10.1016/10.3389/fcell.2024.1347616.
[73] L. Feng, X.-B. Jia, F. Shi, Y. Chen, Identification of Two Polysaccharides from *Prunella vulgaris* L. and Evaluation on Their Anti-Lung Adenocarcinoma Activity, Molecules, 15 (2010) 5093-5103, https://doi.org/10.1016/10.3390/molecules15085093.
[74] V. Russo, L. Falco, V. Tessitore, A. Mauriello, D. Catapano, N. Napolitano, M. Tariq, A. Caturano, G. Ciccarelli, A. D'Andrea, A. Giordano, Anti-Inflammatory and Anticancer Effects of Anticoagulant Therapy in Patients with Malignancy, Life (Basel, Switzerland), 13 (2023), https://doi.org/10.1016/10.3390/life13091888.
[75] R.P. Santos, A.M.F. Tovar, M.R. Oliveira, A.A. Piquet, N.V. Capillé, S. Oliveira, A.H. Correia, J.N. Farias, E. Vilanova, P.A.S. Mourão, Pharmacokinetic, Hemostatic, and Anticancer Properties of a Low-Anticoagulant Bovine Heparin, TH open : companion journal to thrombosis and haemostasis, 6 (2022) e114-e123, https://doi.org/10.1016/10.1055/s-0042-1745743.
[76] N.S. Key, A.A. Khorana, N.M. Kuderer, K. Bohlke, A.Y.Y. Lee, J.I. Arcelus, S.L. Wong, E.P. Balaban, C.R. Flowers, L.E. Gates, A.K. Kakkar, M.A. Tempero, S. Gupta, G.H. Lyman, A. Falanga, Venous Thromboembolism Prophylaxis and Treatment in Patients With Cancer: ASCO Guideline Update, J Clin Oncol, 41 (2023) 3063-3071, https://doi.org/10.1016/10.1200/jco.23.00294.